

# Interacting binaries W Serpentids and Double Periodic Variables

R.E. Mennickent<sup>1</sup>\*, S. Otero<sup>2</sup>, Z. Kołaczowski<sup>3</sup>

<sup>1</sup>Universidad de Concepción, Departamento de Astronomía, Casilla 160-C, Concepción, Chile

<sup>2</sup>Buenos Aires, Argentina; American Association of Variable Star Observers (AAVSO), Cambridge, MA, USA

<sup>3</sup>Instytut Astronomiczny Uniwersytetu Wrocławskiego, Kopernika 11, 51-622 Wrocław, Poland

## ABSTRACT

W Serpentids and Double Periodic Variables (DPVs) are candidates for close interacting binaries in a non-conservative evolutionary stage; while W Serpentids are defined by high-excitation ultraviolet emission lines present during most orbital phases, and by usually showing variable orbital periods, DPVs are characterized by a long photometric cycle lasting roughly 33 times the (practically constant) orbital period. We report the discovery of 7 new Galactic DPVs, increasing the number of known DPVs in our Galaxy by 50%. We find that DPVs are tangential-impact systems, i.e. their primaries have radii barely larger than the critical Lubow-Shu radius. These systems are expected to show transient discs, but we find that they host stable discs with radii smaller than the tidal radius. Among tangential-impact systems including DPVs and semi-detached Algols, only DPVs have primaries with masses between 7 and 10  $M_{\odot}$ . We find that DPVs are in a Case-B mass transfer stage with donor masses between 1 and 2  $M_{\odot}$  and with primaries resembling Be stars. W Serpentids are impact and non-impact systems, their discs extend until the last non-intersecting orbit and show a larger range of stellar mass and mass ratio than DPVs. Infrared photometry reveals significant color excesses in many DPVs and W Serpentids, usually larger for the latter ones, suggesting variable amounts of circumstellar matter.

**Key words:** stars: early-type, stars: evolution, stars: mass-loss, stars: emission-line, stars: variables-others

## 1 INTRODUCTION: UNSOLVED PROBLEMS IN BINARY STAR EVOLUTION

Since most stars in the universe are binaries or members of gravitationally bounded systems, binary star evolution constitutes a primordial subject for understanding large stellar populations. The case of intermediate-mass binaries of the Algol type is especially interesting since epochs of severe interaction must exist to account for the mass ratio distribution (Sarna 1993, Van Rensbergen et al. 2011, de Mink et al. 2014). In spite of the importance of the binary interaction stage, is not clear how efficient the processes of mass and angular momentum transfer are, remaining unknown how much matter is deposited into the interstellar medium and how much is accreted by one of the stellar components.

For the above reasons the identification and study of heavily interacting binaries is important to bring clues on the nature of mass loss mechanisms during epochs of binary interaction. Two classes of interacting binaries (IBs) showing evidence of interaction are relevant in this sense: the Double Periodic Variables (DPVs) and the W Serpentis stars. They are both members of the more general class of Algols, close binaries usually consisting of a cool evolved star and a main sequence early type star. Early in its history, the

secondary star would have been more massive, and evolved first until overfilling its Roche lobe. After fast mass exchange, the lobe-filling star became the less massive of the pair (e.g. Eggleton 2006).

Double Periodic Variables are semi-detached interacting binaries showing a long photometric periodicity lasting about 33 times the orbital period (Mennickent et al. 2003); a couple of them have been found in the Galaxy (Mennickent et al. 2012a) and more than one hundred fifty in the Magellanic Clouds (Poleski et al. 2010, Pawlak et al. 2013). An inherent feature of DPV is presence of relatively large and optically thick circumprimary disc. The long-cycle has been interpreted as evidence for cyclic mass loss (Mennickent et al. 2008), probably through a modulated disc-wind (Mennickent et al. 2012b). Surprisingly, in spite of evidence for mass loss, the orbital period remains remarkably constant in all well studied DPVs (e.g. Mennickent et al. 2012a, Mennickent 2014, Barria et al. 2013, Garrido et al. 2013).

W Serpentis stars are interacting binaries consisting of a hot star surrounded by an optically thick accretion disc (Plavec 1980a,b, 1982, Young & Snyder 1982). The W Serpentids are characterized by strong ultraviolet emission lines of highly excited species like He II, C II, Al III, Fe III, C IV, Si IV and N V seen at every orbital phase, that have been thought to be formed in a super corona produced by the process of mass transfer and accretion (Plavec, Weiland & Koch 1982) or by scattering in an induced stel-

\* E-mail: rmennick@astroudec.cl

lar wind (Plavec 1989). In addition, the light curve tends to be noisy and the orbital periods variable. The W Serpentids have been interpreted as semi-detached close binaries with circumprimary discs fed by Roche-lobe overflow at mass transfer rates larger than normal Algols (Plavec 1989).

The orbital eccentricity in DPVs and W Serpentis stars is always compatible with zero; in very few cases is very small and consistent with the effects produced by the mass streams in the radial velocities of close binaries (Lucy 2005). This condition is in agreement with the theoretical prediction of a rapid orbit circularization for these systems by dynamical tides (Zahn 1975, 1977).

The main goal of this paper is to compare, for the first time, DPVs with W Serpentids from the observational point of view, trying to clarify if they are two separated classes of interacting binaries, and if they are related from an evolutionary perspective. We also present a new census of Galactic DPVs, presenting 7 new systems, increasing significantly the number of these objects in our Galaxy.

The paper is organized as follow: in Section 2 we present our methodology for searching for new DPVs and give sources for infrared photometric data. In Section 3 the results of this search are presented, along with a compilation and analysis of DPV and W Serpentids data found in the literature. In this section we also analyze 2MASS and WISE colors for the sample stars. In Section 4 a discussion of our results is presented. We finish with our conclusions in Section 5.

## 2 METHODOLOGY AND DATA SOURCES

### 2.1 Search for new Galactic Double Periodic Variables

The new DPVs presented in this study were found by one of us (S.O.) as part of a multi-survey variable star search using three publicly available databases: the All Sky Automated Survey - ASAS-3 (Pojmanski 2002), the Northern Sky Variability Survey - NSVS (Wozniak et al. 2004) and the Hipparcos Catalogue (Perryman et al. 1997). More than 3000 new variable stars were found and hundreds of new/revised classifications of known variables were made. Here we report the discovery of 7 new galactic DPVs, clearly distinguished by their blueish colors, two periods and characteristic period ratio.

### 2.2 Period determination and light curve disentangling

The photometric periods of new DPVs were determined with the IRAF PDM task (Stellingwerf 1978). Then we disentangled the two main photometric frequencies by using a code specially designed for this purpose (e.g. Mennickent et al. 2012a). The code adjusts the orbital signal with a Fourier series consisting of the fundamental frequency plus its harmonics. Then it removes this signal from the original time series letting the long periodicity present in a residual light curve. The program fits this remaining signal with another Fourier series consisting on fundamental frequency and harmonics and remove it. As result we obtain the cleaned light curve with no additional frequencies and two light curves for the isolated orbital and long periods.

### 2.3 W Serpentis stars in the literature

While DPV publications are relatively recent and we can easily find data in the literature for a statistical analysis, data for W Serpentids

are more disperse and not so easily accessible; a brief description of these data is given below.

We searched for physical data of W Serpentids in the literature, starting with the catalog of Peculiar Emission Line Algols of Gudel & Elias (1996). However, we found that several of their objects proposed as W Serpentids are of other nature and were not included in our analysis. Here we provide a list of these objects in order to avoid confusion in future investigations. RZ Sct is proposed as a double contact binary (Olson & Etzel 1994),  $\phi$  Leo (14 Leo = HD 83808) is an evolved Am binary (Griffin 2002), V644 Mon, KX And and AX Mon are long period Be star binaries (Halbedel 1989, Tarasov, Berdyugina & Berdyugin 1998, Puss & Leedjarv 1997) and SS Cam an eclipsing RS CVn system (Arnold et al. 1979). In addition, after searching the ADS we find that in the long-period Algols WW And, KU Cyg, RX Gem, DN Ori, AY Per, the Algols with cyclic period changes WW Cyg, SW Cyg and Y PsC, and the binaries SY And, UZ Cyg, RW Gem, TX UMa, TU Mon, U CrB, AM Aur and 14 Ser, there is no reported evidence for a W Serpentis type classification. Finally, AU Mon is a Double Periodic Variable discussed in this paper and RW Tau ( $P_o = 2.77$  days with variable period changes, Simon 1977, no physical data available) is classified as a weak W Serpentis star probably related to transitional objects like V356 Sgr and U Cep (Plavec & Dobias 1983).

The remaining 6 systems in the Gudel & Elias catalog, truly classified as W Serpentids, were investigated for fundamental system and stellar parameters in the literature, viz., RX Cas, SX Cas, V367 Cyg, RY Per, W Ser and RS Cep. We added UX Mon, W Cru and BY Cru from the list of W Serpentids by Wilson et al. (1984) and also added the prototype of the class  $\beta$  Lyrae, amounting to 10 W Serpentis stars.

The following stars have been mentioned as possible W Serpentids in the literature but they are not included in this work for the reasons given below: V453 Sco (HD 163181) only shows high excitation UV emission lines at orbital phase 0.6 (Hutchings & Van Heteren 1981), BM Cas is a binary in a common envelope phase (Pustynnik, Kalv & Harvig 2007), U Cep, KU Cyg, RZ Oph and V356 Sgr are classified as transition objects by Plavec (1989). For V1507 Cyg (HD 187399) we did not find reports of ultraviolet emission lines, whereas AG Peg and AR Pav are symbiotic binaries (Yoo 2008, Quiroga et al. 2002, respectively). Finally, HD 207739 shows variable ultraviolet emission and probably is a transition object (Kondo, McCluskey & Parsons 1985).

### 2.4 Three systems previously classified as DPV candidates

In a recent paper, Mennickent & Rosales (2014) report the discovery of two new Galactic DPVs, viz. V495 Cen and V4142 Sgr, which are included in this paper. In addition, they classified as DPV candidates the following objects, due to the presence of two photometric periods in their ASAS light curves: TYC 6083-192-1, TYC 8638-2548-1 and UX Cnc. However, due to their very long periods, of duration comparable with the time baseline, their small long-cycle amplitudes and very red colors, we argue for a RS CVn nature for these systems, where the long cycle probably represents cycles of sunspot-like activity. In this view, the short periods reported previously for these objects are twice the true rotational periods of a single RS CVn star. Let's discuss briefly each of these systems.

TYC 6083-192-1 is classified as E/RS with Coronal Activity in the ASAS Eclipsing Binaries Catalogue (Szczygiel et al. 2008) and published spectra indicate a K4V+MOV system (Parihar et al.

**Table 1.** Orbital and long-cycle ephemerides determined in this paper for 7 new DPVs and TYC 7398-2542-1.

System	$P_o$ (d)	HJD <sub>o</sub> (245 0000 +)	$P_l$ (d)	HJD <sub>l</sub> (245 0000 +)
BF Cir	$6.4592 \pm 0.0003$	$1905.1538 \pm 0.0323$	$219 \pm 2$	$1846.83 \pm 3$
CZ Cam	$8.055 \pm 0.015$	$7871.4039 \pm 0.3222$	$267 \pm 3$	$5771.00 \pm 8$
HD 151582	$5.823 \pm 0.003$	$1930.6928 \pm 0.1165$	$160 \pm 2$	$1779.02 \pm 4$
HD 256413	$6.775 \pm 0.004$	$2616.9967 \pm 0.2032$	$242 \pm 12$	$2621.77 \pm 20$
V761 Mon	$7.754 \pm 0.002$	$1868.7884 \pm 0.0775$	$268 \pm 2$	$1699.54 \pm 3$
TYC 7398-2542-1	$2.76903 \pm 0.00002$	$1953.8027 \pm 0.0055$	$106 \pm 1$	$1874.99 \pm 5$
TYC 8627-1591-1	$7.462 \pm 0.001$	$1884.9720 \pm 0.3731$	$268 \pm 3$	$1654.21 \pm 5$
V1001 Cen	$6.736 \pm 0.003$	$2441.9293 \pm 0.1347$	$247 \pm 3$	$2439.69 \pm 5$

2009). Additionally, the SAO catalogue (Whipple 1966) indicates a spectrum K7 and it is classified as K5 in the FOCAT-S catalogue (Bystrov et al. 1994). The reported short period of 90.4 days assumed eclipses much wider than usual for RS CVn binaries and it could be twice the stellar rotational period of 45.2 days. The long cycle of around 3497 days implies a period ratio of about 77, much different from a typical DPV period ratio.

TYC 8638-2548-1 is a ROSAT X-ray source with  $J - K = 0.79$  and  $B - V = 1.13$ . The long cycle shows an asymmetrical light curve as most RS CVn systems. The reported short period of 101.3 days assumes eclipses, much wider than usual for RS CVn binaries, and could be twice the stellar rotational period of 50.65 days. The long period of about 3400 days implies a period ratio of 67.1, unusual for a DPV.

UX Cnc with  $J - K = 0.69$  and  $B - V = 1.03$ , seems to be another RS CVn. The reported short period of 84.8 days assumes eclipses, much wider than usual for RS CVn binaries, and could be twice the stellar rotational period of 42.24 days. The suggested long cycle of 2158 days implies a period ratio of 51.1, unusual for a DPV.

For the above reasons the three aforementioned systems were not included in our census of Galactic DPVs.

## 2.5 2MASS and WISE infrared data

Here we give a brief summary of the infrared photometry used in this paper. The query for magnitudes of the DPVs and W Serpentids was done through the NASA/IPAC infrared science archive<sup>1</sup> and focused on two infrared imaging surveys.

Firstly, we scanned for data obtained with the Two Micron All Sky Survey (2MASS), a project that uniformly scanned the entire sky in three near-infrared bands,  $J$  at  $1.25 \mu\text{m}$ ,  $H$  at  $1.65 \mu\text{m}$  and  $K_s$  at  $2.17 \mu\text{m}$ , to detect and characterize point sources brighter than about 1 mJy in each band, with signal-to-noise ratio (SNR) greater than 10, using a pixel size of  $2.0''$  (Skrutskie et al. 2006). The Infrared Processing and Analysis Center (IPAC) is responsible for all data processing through the Production Pipeline, and construction and distribution of the data products. Magnitude limits for point sources are at least 15.8, 15.1 and 14.3 mag at  $J, H, K$  bands, respectively. 2MASS successfully obtained photometry of sources as bright as  $K \sim 4$  mag measuring the flux at the wings of the stellar image of bright stars. Unconfused point sources (with  $\text{SNR} \gg 20$ ) have a photometric accuracy of better than 3%.

Secondly, we searched for magnitudes obtained with The Wide-field Infrared Survey Explorer (WISE), a NASA medium

class explorer mission that conducted an all-sky survey at mid-infrared bandpasses centered around wavelengths 3.4, 4.6, 12 and  $22 \mu\text{m}$  (hereafter  $W1, W2, W3$  and  $W4$ ; Wright et al. 2010). The survey was conducted with a 40 cm cryogenically-cooled telescope in sun-synchronous polar orbit. Four infrared detectors imaged the same sky field of view during 7.7 s ( $W1, W2$ ) and 8.8 s ( $W3, W4$ ). We use here the data of the second-pass processing, obtained with improved calibration and processing algorithms, superseding those obtained for the preliminary data release. Sources in the All-Sky Release Source Catalog saturate the WISE detectors at characteristic magnitudes of 8.1, 6.7, 3.8 and -0.4 mag in  $W1, W2, W3$  and  $W4$ , respectively. Profile-fitting photometry extracts reliable measurements of saturated sources using the non-saturated wings of their profiles up to brightnesses of  $\approx 2.0, 1.5, -3.0$  and  $-4.0$  mag in  $W1, W2, W3$  and  $W4$ .

The analysis of 2MASS and WISE magnitudes is presented in Section 3.6.

## 2.6 About stellar and disc parameters.

Since our work relies on a compilation of data available in the literature, some words are necessary about the methods that have been utilized to obtain the stellar and disc parameters of the systems under study.

Parameters for DPVs are more homogeneously determined than in W Serpentids. In most cases the light curve was modeled with a code created by Djurašević (1992a,b). The code uses the inverse-problem solving method based on the simplex algorithm, and the model of a binary system with a disc. Spectroscopically derived data (for instance temperature of the donor or the system mass ratio) are usually used as input to constrain the light curve solution. Stellar and disc parameters and their errors are provided by the authors as the formal solution of the aforementioned model. In particular, the stellar flattening due to rotation is included and the radius equivalent of a spherical star of the same volume is provided. Due to the use of the same methodology in 6 of 7 cases, we don't expect large systematic errors in DPV stellar and disc parameters.

The situation is different for W Serpentis stars. The method described in the paragraph above was used only for one of the W Serpentis stars in our sample (10%), to determine stellar parameters, and for 3 of them to determine disc parameters (30%). In all other cases different methods were used and hard-to-quantify systematic errors are likely present. In particular, the hiding of the primary by the disk makes difficult to detect it in the spectrum. Sometimes the radial velocities for the primary are non-existent or affected by complex absorption/emission line components. These components comes from the disc and the gas stream and can reveal unknown effects of variable optical depth. In the worst cases the

<sup>1</sup> <http://irsa.ipac.caltech.edu/Missions/wise.html>

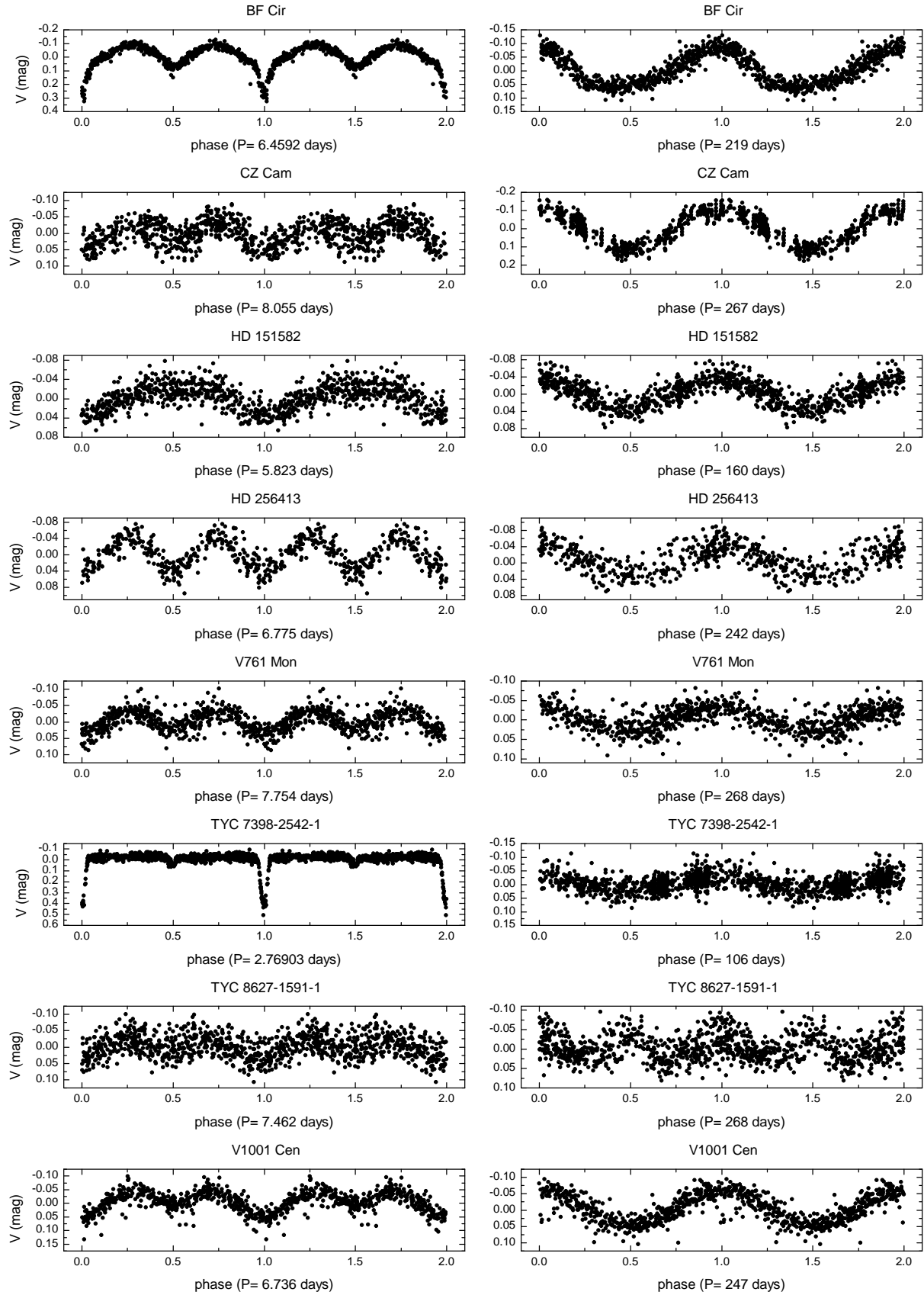


**Figure 1.** Disentangled orbital and long-cycle light curves for the 7 new DPVs presented in this paper and the eclipsing binary TYC 7398-2542-1 (ASAS J182841-3314.6). They are phased according to the ephemerides given in Table 1.

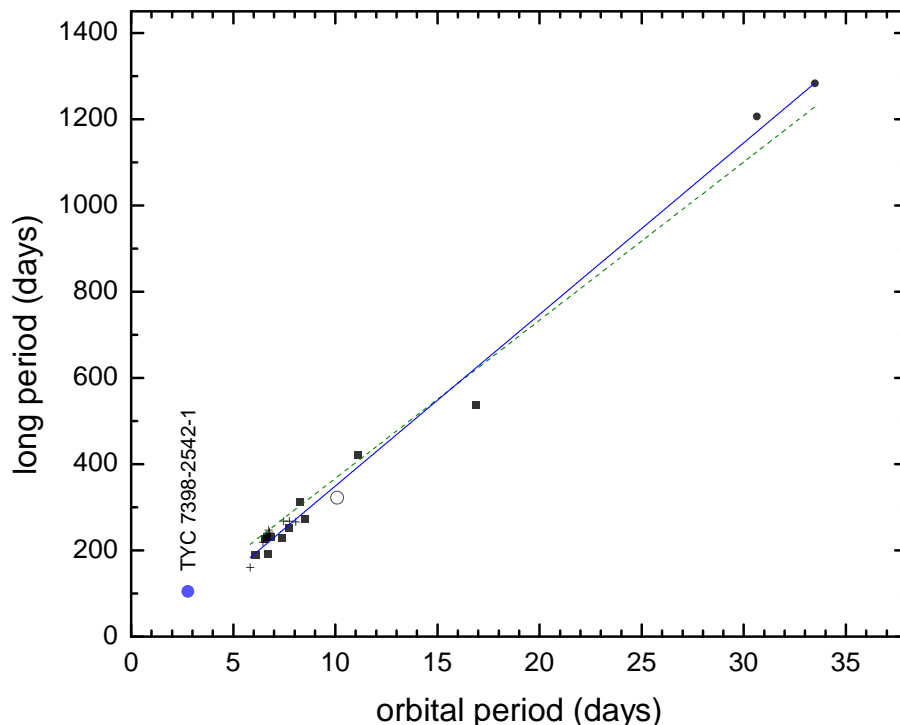


**Figure 2.** Orbital and long-cycle period for Galactic Double Periodic Variables and the eclipsing binary TYC 7398-2542-1. The 7 new DPVs presented in this paper (pluses) are included with those by Mennickent & Rosales (2014; filled circles) and those by Mennickent et. al. (2012a, squares), along with V360 Lac (Hill et al. 1997, open circle). The best linear fits determined by least square fitting are also shown; one is forced to pass by the origin (dashed line) and the other has the best intersection in the y-axis (solid line).

temperature for the primary is estimated from the  $U - B$  or  $B - V$  colors, and a main sequence stage is assumed along with a mass-radius relationship. For the above reasons, although we include the formal errors provided by the authors, we can expect larger systematic effects for the parameters of the studied W Serpentis stars.

## 2.7 About evolutionary models

We provide for most DPVs the age and the mass transfer rate as found in the literature. They were usually determined by comparison of observed quantities, in particular the orbital period, stellar masses, radii and luminosities, with the predictions of the binary evolution models of Van Rensbergen et al. (2008). These models include cases of strong and weak tidal interaction and also some non-conservative evolutionary tracks. A multi-parametric  $\chi^2$  minimization is done between observed and predicted quantities, in order to obtain the best model for every system, as described by Mennickent et al. (2012a). Although formal errors are provided by the authors, the limited grid of models and ad-hoc assumption of mass loss in the non-conservative cases, are intrinsic limitations of the method.

## 3 RESULTS

### 3.1 The new Double Periodic Variables

The result of our search for new Galactic Double Periodic Variables was the discovery of 7 new DPVs whose relevant information is given in Table 1 and light curves shown in Fig. 1. Ephemerides refers to the minimum of the orbital light curve and maximum

brightness of the long-cycle light curve. During our research we found the object TYC 7398-2542-1 (ASAS J182841-3314.6) as a DPV candidate with  $P_o = 2.76903 \pm 0.00002$  days and  $P_l = 106 \pm 1$  day. However, we reject the DPV classification since the light curve is of detached type (all others DPVs are semi-detached type) and the orbital period is quite short (all other DPVs have  $P_o$  longer than 5 days). The long period of this object could be due to an unresolved variable companion. The confirmed new DPVs are: BF Cir, the only eclipsing one, HD 151582 showing a single-wave orbital light curve and CZ Cam, HD 256413, HD 58645, TYC 8627-1591-1 and V1001 Cen showing double-wave ellipsoidal orbital variability. All long-cycle light curves are single-hump except that of TYC 8627-1591-1 showing a double-wave modulation.

The number of currently known Galactic DPVs amounts to 21; they are presented in Table 2, along with their orbital periods (ranging from 5.8 to 33.5 days), long periods (ranging from 160 to 1283 days), period ratios, spectral types and extreme visual magnitudes. From the published spectral types of DPVs, it is notable the presence of an early B-type component in most systems.

The orbital and long periods of DPVs follow an almost linear tendency (Fig. 2). The best linear fit passing by the origin is:

$$P_l = (36.7 \pm 0.7)P_o, \quad (1)$$

with  $rms = 38$  days. This relation is slightly different than previously reported with only 13 systems in the Galaxy, viz.  $P_l = (32.7 \pm 0.9)P_o$  (Mennickent et al. 2012a) or  $P_l = 33.13P_o$  for 125 DPVs in the Large Magellanic Cloud (Poleski et al. 2010). Excluding the two longest periods we find  $P_l = (33.4 \pm 0.6)P_o$  with  $rms = 22$  days, therefore the difference comes primarily from those systems. Since equation (1) gives oddly displaced residuals, we can get a better fit for the data with:

$$P_l = (-48.7 \pm 10.6) + (39.8 \pm 0.8)P_o, \quad (2)$$

with  $rms = 27$  days. The distribution of period ratios shows a mean of 33.9 with a standard deviation of 3.1 and minimum and maximum values of 27.48 days and 39.36 days (Fig. 3). We notice that the above relationships still remain limited by the low number of objects and likely by observational selection.

### 3.2 Physical data of DPVs

Physical parameters of all relatively well studied DPVs, 6 in our Galaxy and 1 in the LMC, are given in Table 3. We calculated luminosities using the published bolometric magnitudes, except for V360 Lac, where we used average stellar radii and temperatures and the relationship  $L = 4\pi\sigma^2 R^2 T^4$ . All DPV light curves have been modeled with an accretion disc around the more massive component, except those of V360 Lac and LP Ara. The fact that no disc was assumed in the V360 Lac configuration could produce a bias in the system parameters and mimic a near contact configuration (Linnell et al. 2006). On the other hand, LP Ara light curve has been modeled with a Wilson-Devinney code constraining the light contribution of a possible accretion disc to less than 5% of the total orbital light (Mennickent et al. 2011). It is then very likely that all DPVs harbor accretion discs. The evolutionary stage of some DPVs has been found comparing the system parameters with those of a grid of published evolutionary tracks allowing to obtain the system age, mass transfer rate and core hydrogen concentration for the cool and hot star of the binary pair ( $X_c$  and  $X_h$  in Table 3).

An inspection of Table 3 reveals that whereas donors of DPVs span a considerable range of effective temperatures and spectral types, between 5.7kK to 12.9kK, the gainers cluster around early B-type stars ( $T_{eff}$  between 15.9kK and 25.1kK), consistent with the spectral classifications given in Table 2. The range of binary total mass for the DPV phenomenon is 8–13  $M_\odot$ . We find that all systems have reversed their mass ratio and have  $q \lesssim 0.3$ .

It is notable that all DPVs are practically in a full Case-B mass transfer state with almost zero hydrogen in the donor core ( $X_c \approx 0$ ). Consequently, the donor is evolved, filling its Roche lobe, and all systems with determined ages have been found inside or after a mass transfer rate event (see references in Table 3). The evolutionary stage inferred from the models, inside or slightly after a mass transfer event, is compatible with the observational evidence of circumstellar matter and accretion discs in DPVs.

Another interesting aspect of Table 3 is that according to the listed references, the best models are found at a conservative stage. If the DPV phenomenon is due to cyclic mass loss as proposed by Mennickent et al. (2008), then this conservative character of the models could indicate that the departure from the conservative case is probably subtle, i.e. the mass loss is minor compared with the accreted mass in these systems. Alternatively, it could mean that the system has entered the non-conservative phase just recently, something already envisaged for AU Mon (Mennickent 2014). Moreover, an earlier liberal age of large mass transfer with substantial mass loss is probably discarded because of the good match with conservative (or slightly non-conservative) models.

### 3.3 Physical data of W Serpentids

We present in Tables 4 and 5 the physical data of W Serpentis stars. The luminosities are calculated from the bolometric magnitudes, except for BY Cru, W Cru and RS Cep where we used average stellar radii and temperatures provided by the authors and the relation-

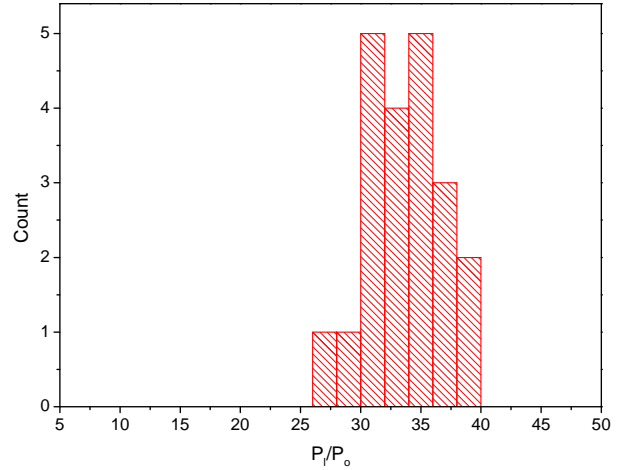


Figure 3. Histogram of period ratios for Galactic DPVs.

ship  $L = 4\pi\sigma^2 R^2 T^4$ . We find that W Serpentids are characterized by secondary star masses between 0.4 and 3.9  $M_\odot$ , and primary star masses between 2.8 and 16.2  $M_\odot$ . Total mass in W Serpentids, between 2.5 and 16.2  $M_\odot$ , can be smaller than for DPVs. The mass ratios of W Serpentids span a larger range than DPVs, from 0.15 to 1.2, they are lower than 1.0 except for UX Mon (1.15). The temperatures of the secondary also have larger range than DPVs, from 4kK to 13kK. Contrary to DPVs, W Ser are characterized by changing orbital periods (it increases or decreases a couple of seconds per year) and higher mass transfer rates of the order of  $10^{-5}$  to  $10^{-8} M_\odot \text{yr}^{-1}$ . These figures are usually obtained from the rate of orbital period change, assuming conservative evolution. The orbital periods run from 5.9 days (UX Mon) to 198.5 days (W Cru). In our sample of DPVs and W Serpentids, the longer orbital periods are found in W Serpentis stars.

Contrary to previous reports (Sudar et al. 2011), we find a constant orbital period in UX Mon. The epoch of minimum published in 1950 (HJD 2433328.853; Kreiner and Ziolkowski 1978) was still valid in 2009 (epoch of ASAS-3 data) after 59 years and the best period fitting the ASAS V-band light curve is  $5.90442 \pm 0.00005$  d. The previous reports of period changes might have been influenced by measurements of eclipse timings in a light curve of variable shape. Disentangling the light curve in an orbital and non-orbital component, we find short-term and non-periodic residual variability with amplitude of about 0.2 mag (Fig. 4). Since this variability decreases during primary minimum and just before secondary eclipse, it likely arises from structures in the orbital plane and inside the binary, like the accretion disc and hotspot.

### 3.4 DPVs and W Serpentids are different classes of objects

Apart from the physical parameters discussed in the previous sections, suggesting significant differences between W Serpentids and DPVs, there are also differences from the observational point of view.

For instance, none W Serpentids has been found with a long photometric cycle matching the relationship given by Eq. 1. There are long cycles in some W Serpentids; in  $\beta$  Lyr a period of 282.4 d is reported (Harmanec et al. 1996) and in RX Cas the long cycle lasts 516.1 days (Kalv 1979). For the  $\beta$  Lyr the period ratio is 21.8 and for RX Cas 16.0, they do not fit the period-period relationship of DPVs.

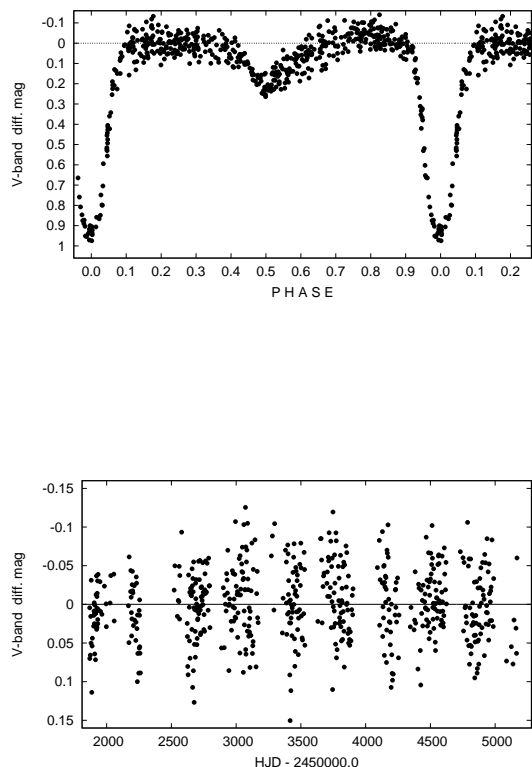


**Figure 4.** (up): Disentangled ASAS light curve for UX Mon fitted with a single period of 5.90442 d. (below): residual light curve showing additional short-term variability with total amplitude of about 0.2 mag.

A search in the Mikulski Archive for Space Telescopes (MAST<sup>2</sup>) revealed that only 3 of the DPVs presented in this paper (V393 Sco, AU Mon and V360 Lac) have IUE<sup>3</sup> ultraviolet spectra. Searching the existing literature we confirmed that they do not fit the W Serpentid definition of showing UV emission lines at all orbital phases, suggesting furthermore that DPVs and W Serpentids are two distinct types of objects.

### 3.5 Comparison with semi-detached Algols

We compare luminosities, masses and temperatures of primaries and secondaries of W Serpentids, DPVs and semi-detached Algols (Fig. 5), using as reference the loci for the main sequence for  $Z = 0.02$  and some evolutionary tracks for single stars from Pols et al. (1998). These are included to illustrate the degree of donor evolution, not to represent their evolutionary track, since it differs for a member of a mass-transferring binary, as illustrated by the binary track in the same panel (see Section 4.2). It is clear that DPVs and W Serpentids generally possess hotter, more massive and more luminous stellar components than semi-detached Algols. In addition,

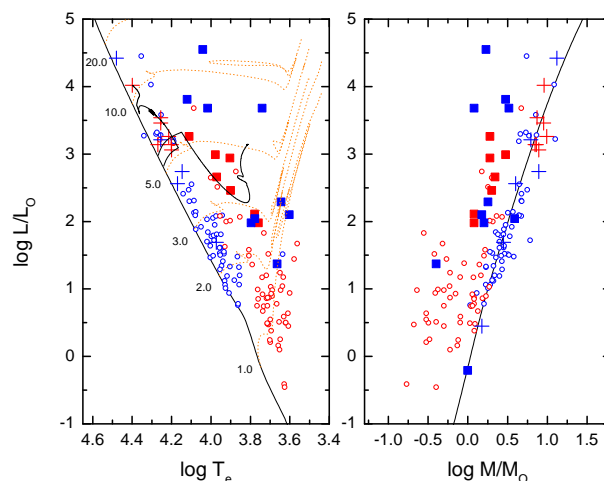


**Figure 5.** Comparison of physical data for semi-detached Algols from Dervişoğlu, Tout & Ibanoglu (2010, primaries open blue circles and secondaries open red circles), DPVs (primaries red crosses and secondaries red squares) and W Serpentids (primaries blue crosses and secondaries blue squares). The zero-age main sequence for  $Z = 0.02$  is plotted with a solid black line and evolutionary tracks for single stars with initial masses (in solar masses) labeled at the track footprints are also shown (Pols et al. 1998). The best evolutionary tracks for the primary and secondary of HD 170582 are also plotted by two solid lines in the left panel (see text for details).

primaries are slightly evolved, slightly displaced from the main sequence in the  $\log L$  vs.  $\log T_{eff}$  diagram, as occurs in Algols but secondaries are quite evolved and do not follow the mass-radius relationship as occurs for primaries. This has been traditionally interpreted as the result of the evolution of a donor that has transferred part of its atmosphere onto the gainer resulting in a much evolved cooler star whereas the gainer remains near the main sequence (e.g. Dervişoğlu, Tout & Ibanoglu 2010). It seems that some donors of W Serpentids are slightly more evolved than DPV donors. When doing this comparison, we should keep in mind that catalogues of Algols might still contain some DPVs or W Serpentids. For instance, Budding et al. (2004) classify as Algol 2 of our 5 Galactic DPVs and 5 of the 10 W Serpentids mentioned in this paper.

Another aspect of Fig. 5 is the gap in donor luminosity between W Serpentids and DPVs; these latter occupy an intermediate region between faint and bright W Serpentid donors. Due to the limited dataset, this tendency could be an artifact.

### 3.6 Infrared excess and circumstellar matter

#### 3.6.1 2MASS photometry of DPVs and W Serpentids

2MASS colors were obtained from SIMBAD for our DPVs and W Serpentids. A sample of Be stars with measured  $JHK$  colors was included as comparison; data are from Howells et al. (2001) who present infrared photometry of 52 isolated Be stars of spectral types O9-B9 and luminosity classes III-V. The purpose of including Be stars is that they are fast B-type stars surrounded by ejected disc-like circumstellar envelopes, hence they provide a reference for evaluating the effects of circumstellar material in the infrared colors of our sample stars. We also included in our study theoretical colors for dwarfs and giants obtained from Bessell et al. (1998). We did not apply interstellar extinction corrections since for most objects there is no distance estimated. However, interstellar extinction is small in infrared wavelengths and it is expected to have a

<sup>2</sup> <https://archive.stsci.edu/index.html>

<sup>3</sup> <http://science.nasa.gov/missions/iue/>



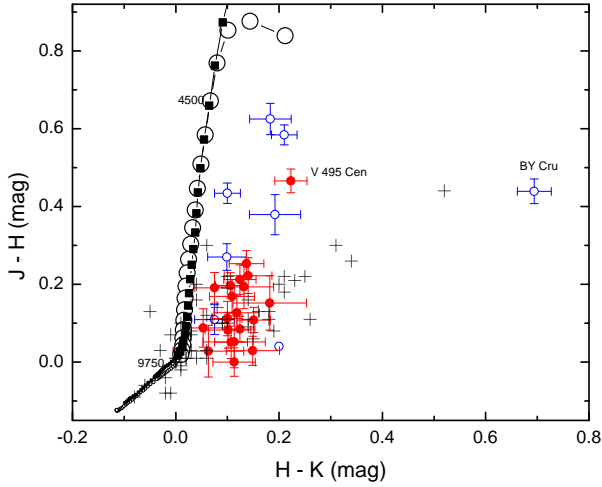


**Figure 6.** Color-color diagram for Galactic DPVs (red filled circles), W Ser stars (blue open circles), Be stars (crosses, data from Howells et al. 2001) and synthetic stellar atmosphere models with  $\log g = 4.0$  (squares with lines) and  $\log g = 3.0$  (open circles with lines, from Bessell et al. 1998). The effective temperature of 2 selected synthetic models have been labeled.

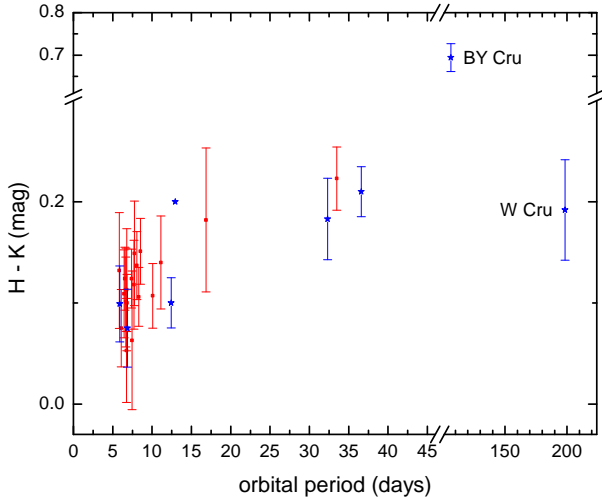


**Figure 7.** 2MASS  $H - K$  color versus orbital period for DPVs (red squares) and W Serpents (blue stars).

small contribution to the color excess compared with circumstellar reddening.

The infrared colors of the studied stars indicate that all these stars show color excess in comparison with the main sequence and giant stars, and that W Serpents stars in general show redder color than DPVs (Fig. 6). Interestingly, Be stars occupy the same color range as DPVs. Since Be stars show color excess mostly attributed to circumstellar reddening and proportional to Balmer emission line strength (Howells et al. 2001, Dachs et al. 1988), it is reasonable to assume that the color excess observed in DPVs is also a signature of circumstellar matter, the same for W Serpents showing even larger color excess.

We also find that longer orbital period systems tend to show redder  $H - K$  colors (Fig. 7). This might be related to the presence of bigger and more luminous secondaries in longer period systems, but also to larger accretion discs inside the large Roche lobes of the primaries.

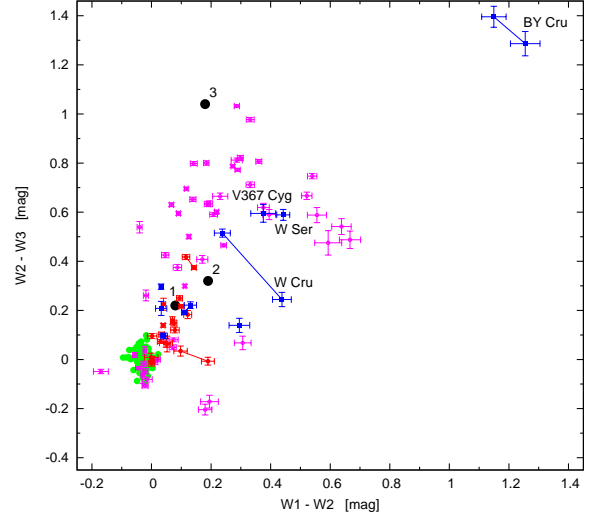


**Figure 8.** WISE colors for single and non-variable HIPPARCOS stars spanning the spectral-type range B1 V to K3 V (green dots), DPVs (red dots), Be stars (magenta circles) and W Serpents stars (blue squares). Different epochs for a given star are represented by points joined by a line. The error bars represent variance of the mean; the observational amplitude of variability can be several times larger. The big black dots labeled with numbers refers to the models discussed in the text.

### 3.6.2 WISE photometry of DPVs and W Serpents

We visually inspected the WISE images at bands W1, W2, W3 and W4 for all systems. In general, all objects were detected at all bands, except some of them at W3 (GK Nor and LP Ara) and W4 (DQ Vel, GK Nor, HD 170582, HD 90834, LP Ara and TYC 8627-1591-1). Presence of nebulosity was not observed.

In order to include most of the objects in our study, we used only the three first WISE magnitudes to construct  $W1 - W2$  and  $W2 - W3$  color indexes. Data obtained during eclipses were discarded. When possible, and just for few cases, we considered independently separated epochs for a given star. In this process some additional epochs were excluded for a given star, due to the lack of simultaneous multi-band data.

We calculated the mean magnitudes for each filter ( $i = 1, 2, 3$ ):

$$W_i = \frac{1}{n} \sum_{j=1}^n w_{i,j}, \quad (3)$$

and the variance of the mean:

$$eW_i = \frac{1}{\sqrt{n(n-1)}} \sqrt{\sum_{j=1}^n (w_{i,j} - W_i)^2}, \quad (4)$$

where mean magnitudes  $W_i$  are defined for samples of  $n$  individual  $w_{i,j}$  magnitudes. These values are given for the sample stars in Tables 6 to 9. We notice that the true variability (measured by the root mean square), can be several times the quoted variance of the mean. As in the case of  $JHK$  photometry, no correction by interstellar reddening was performed. However, at these wavelengths, the effect of interstellar reddening is neglectable.

We compared data of DPVs, W Serpents stars and Be stars; the last were used as testers of circumstellar matter. In addition, we



included as a reference the average colors for 136 main sequence stars from the Hipparcos catalogue. For the selection of this sample we applied several criteria: V magnitude in range of 8 to 10, Hipparcos magnitude ( $H_p$ ) scatter less than 0.04 mag, known variables rejected, only stars with confirmed spectral class V, all known emission line objects were rejected, all known multiple systems were discarded, all stars with very close companions were rejected, finally few outliers were discarded. The final sample consisted of stars in the range of spectral types from B1 V to K3 V (Tables 9 to 11).

From the distribution of systems in the color-color diagram we conclude (Fig. 8): (i) The region occupied by the Hipparcos standards in the range B3 V to K3 V is very compact, around the origin; it means that for binary systems (without IR excess) we can expect exactly the same colors, (ii) DPVs, Be stars and W Serpentis stars show in general significant color excess compared to main sequence stars, (iii) DPVs show in general less color excess than W Serpentids and Be stars, (iv) some DPVs or W Serpentis stars show large color variability and (v) BY Cru stands out showing the largest color excess in our sample (this is also true for the 2MASS  $H - K$  colors).

In order to properly calibrate the color-color diagram with a real physical situation of a close binary similar to the systems considered in this study, we introduce some of the models calculated by Deschamps et al. (2015) for a binary losing matter through a radiative wind formed at the stream-star impact region. Deschamps et al. (2015) use a state of the art code to model the binary parameters during the evolution of the mass transfer episode, focusing on the impact of the outflowing gas and possible presence of dust grains on the spectral energy distribution. Models labeled 1, 2 and 3 in Fig. 8 correspond to models A-df-0.71, B-df-0.71, and B-ld-0.71. These are the models “dust-free” (df) and “low-dust” (ld) at 20 000 yr (model A) and 60 000 years (models B) after peak of mass transfer and with 71% of fraction of the spherical domain covered by the gas outflow (see model details in Deschamps et al. 2015). The models are constructed for a binary consisting of a late G-type giant and a dwarf B-type gainer located at 300 pc.

We interpret the good match of the models 1, 2 and 3 with the position of some DPVs and W Ser stars as evidence of circumstellar matter in these stars. None of the Deschamps et al. (2015) models can reproduce  $W1 - W2$  colors larger than 0.3 mag, neither the  $J - H$  vs.  $H - K$  color distribution of our sample stars; in general the predicted colors are too blue at  $J - H$ . The incapacity of the models in reproducing these regions of the color space could indicate still unexplored model parameters and binary configurations; the complexity of the calculations carried out by Deschamps et al. probably forced the restriction of many parameters to very particular cases. In spite of that, the conclusion that the large color excesses observed in DPVs and especially in W Serpentids can be interpreted as signatures of circumstellar matter seems to be well justified.

We notice that the spectral energy distribution of V393 Sco and HD 170582 in the ultraviolet, optical and infrared ranges has been modeled to high accuracy with the contribution of two stellar components plus interstellar reddening, without necessity of introducing a circumstellar component (Mennickent et al. 2010, Mennickent et al. 2015). This is consistent with the location of both stars in the lower left part of the color-color diagram near the main sequence region; for V393 Sco  $W_1 - W_2 = 0.002$  and  $W_2 - W_3 = 0.0955$  and for HD 170582  $W_1 - W_2 = 0.0786$  and  $W_2 - W_3 = 0.12$ .

Finally we notice that longer orbital period systems tend to show redder  $W_2 - W_3$  colors (Fig. 9). If color excess is a measure

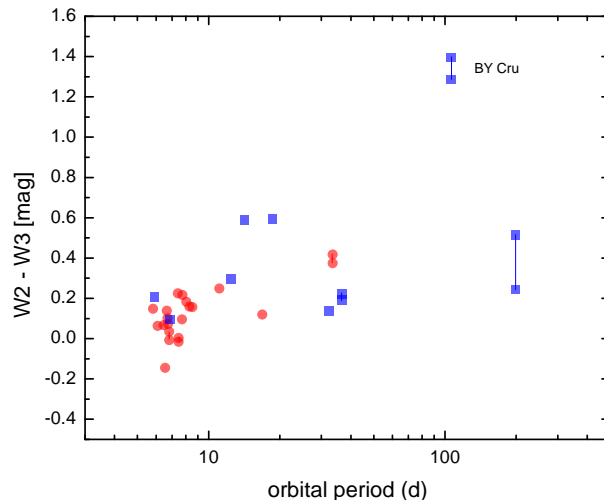


**Figure 9.** WISE colors versus orbital period for DPVs (red dots) and W Serpentis stars (blue squares). Different epochs for a given star are represented by points joined by a line.

of circumstellar matter, as suggested in previous paragraphs, this tendency could reflect the larger Roche lobes and possibly larger discs that these systems can host.

## 4 DISCUSSION

### 4.1 Study of discs in DPVs and W Serpentids

We have compiled disc external radii and gainer radii for DPVs and W Serpentids from the literature (Table 12). These radii relative to the binary separation are shown in Fig. 10. The diagram  $R_1/a$  vs.  $q$  has been previously used to separate Algols with discs and without discs (e.g. Plavec 1989, Peters 2001). Following these authors, we included three theoretical radii in the diagram.

The first one is the Lubow & Shu (1975) critical radius which can be approximated by (Hessman & Hopp 1990):

$$\frac{r_c}{a} = 0.0859q^{-0.426} \quad \text{for } 0.05 < q < 1. \quad (5)$$

which is accurate to 1%. This radius is usually taken as the maximum possible radius of the primary allowing disc formation. A particle orbiting at this radius has the same specific angular momentum as a particle released at the inner Lagrangian point  $L_1$ ; therefore, the radius corresponds to the radial extension of a ring of matter formed by mass loss due to Roche lobe overflow, just before viscosity starts spreading it into a disc. Therefore, a primary whose radius is larger than the critical radius ( $R_1 > r_c$ ) is an impact-system, where the gas stream hits the star and disc formation is unlikely. Actually, due to the finite stream size, still it is possible that the outer stream orbits avoid the impact, the respective radius  $r_{max}$  is a bit larger than  $r_c$  and also a function of the mass ratio (Lubow & Shu 1975). This radius is also shown in Fig. 10.

The third radius considered is the tidal radius (Paczynski 1977, Warner 1995):

$$\frac{r_{tidal}}{a} = \frac{0.6}{1+q} \quad \text{for } 0.03 < q < 1. \quad (6)$$

This radius corresponds to the last non-intersecting orbit; it is assumed that a disc growing larger will start to experience strong shear forces, hence it represents a limit for the disc size.

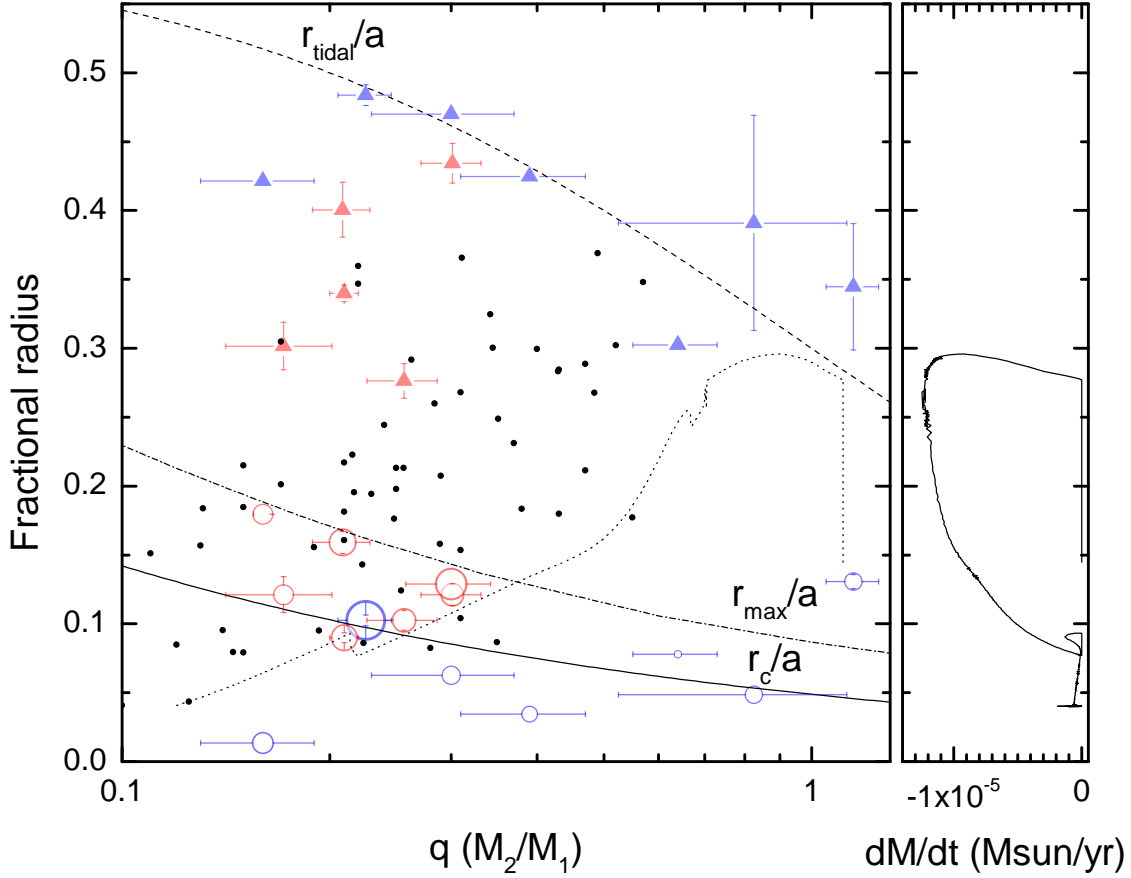


**Figure 10.** The relative radius for the primary ( $R_1/a$ ; red circles for DPVs and blue circles for W Serpentids) and disc ( $R_d/a$ , triangles same color mark), according to the data given in Table 12. Symbol size for stellar radius is proportional to the system total mass. When no  $q$  error was available, we considered a representative error of 14%. Below the circularization radius shown by the solid black line a disc should be formed and below the dash-point a disc might be formed. The tidal radius indicates the maximum possible disc extension (upper dashed line). Semi-detached Algol primaries from Dervişoğlu, Tout & Ibañoğlu (2010) are also shown as black points. The track for  $R_1/a$  for the best model of HD 170582 is shown in the left panel and the corresponding mass transfer rate at the right panel (see text for details).

From the inspection of Fig. 10 and keeping in mind the low number of systems studied, we find that: (i) most DPV primaries are found above the Lubow & Shu (1975) critical radius but below  $r_{max}$ , (ii) W Serpentic gainers have radii normally below the critical radius, (iii) W Serpentic discs usually reach the tidal radius and (iv) DPV discs are smaller than the tidal radius. In this context, we note that a disc twice larger than reported in Table 12 was found by Atwood-Stone et al. (2012) for AU Mon, by modeling the Balmer emission lines. The difference was interpreted by the authors in terms of methods sensible to different disc regions; whereas the fit of emission lines is sensible to optically thin disc regions, the light curve model is sensible to the optically thick disc. Most disc radii in Table 12 are derived from the analysis of light curves and represent the optically thick disc, rather than optically thin Balmer emitting regions.

The finding that DPV gainers are larger than the critical radius but smaller than  $r_{max}$  is a surprising result, since they should be candidates for hosting transient and variable discs (Peters 2001), however we have found that all DPVs have *stable* discs. The position of the DPV gainers in the diagram indicates they are impact systems. However the impact of the stream is almost tangential, probably imparting most of the angular momentum to the star and accelerating it more efficiently than a head-on impact. The fact that

DPVs possess a disc indicates that the disc was formed in spite of the tangential impact. Theoretical work indicates that the impact should rapidly accelerate the star until critical rotation (e.g. Packet 1981). This fact suggests that after critical rotation the extra supplied mass cannot be accumulated on the star, but starts forming an accretion disc in DPVs. The DPV characteristic of having pretty much stable orbital light curves, indicates that these discs, formed in a different way than discs of disc-systems (those with  $R_1 < r_c$ ), are relatively stable. It is possible that rapid rotation favors disc formation (see section 4.1.2). At present, it is not known why these discs are truncated to smaller radii than the tidal radius. The possibility that the disc is formed in earlier epochs, before reaching the tangential-impact condition, is explored at the end of Section 4.2.

The situation for W Serpentic stars is different since with the exception of UX Mon, most of them have primaries smaller than the critical radius, or of similar size. Their discs might be formed in the usual way; the gas stream turns around the star, hits itself forming a hotspot and a ring that subsequently spreads forming an accretion disc. For W Serpentic stars the discs extend almost up to the tidal instability radius. UX Mon is the only W Serpentic with  $q > 1$  and contrary to all others W Serpentic systems, it has a primary much larger than the critical radius; this system could have recently initiated the phase of rapid mass transfer, being still before

the mass-ratio reversal, as suggested by Sudar et al. (2011). Therefore, the system is in a evolutionary stage different from all those considered here.

According to the above arguments, our study would benefit from a comparison with the projected rotational velocities of the primaries. However, the empirical determination of the gainer spin velocity in these systems is very difficult, since the presence of the accretion disc introduces absorption/emission features contaminating the photospheric lines. For instance, optical helium absorptions, potentially good indicators, are quite variable in shape and width during the whole orbital cycle. Something similar happens for ultraviolet lines, especially in W Serpentis stars.

The light curve models described in Section 2.6 cannot discriminate between synchronous or critical rotation of the primary, since it is hidden by the accretion disc. We notice that the use of the equivalent radius of the primary, rather than the equatorial radius in DPVs, might underestimate the parameter  $R_1/a$ . For the extreme case of a critically rotating star the equatorial radius becomes 1.5 times the polar radius (Georgy et al. 2011). Since the equivalent radius is in between both radius, we expect an underestimation of at most 25% in cases of critical rotation (Djurašević G., private communication). This does not invalid the finding of a disc, that has been determined from the light-curve model, which is sensible to the size and shape of the disc rather than the radius of the primary. However, in cases of critical rotation, it should move some DPVs slightly above the  $r_{\max}/a$  limit, i.e. into the region of impact systems. In this region no disc is expected, hence the finding of unexpected stable discs in DPVs remains valid.

#### 4.1.1 A comparison with semi-detached Algols

Among candidate systems to form transient discs, i.e. those with  $r_c < R_1 < r_{\max}$ , we find a clear segregation between Algols and DPVs when plotting the total mass and the mass of the primary for these systems (Fig. 11). The important thing is that DPVs turns to be much more massive than Algols therefore certain range of primary masses are required for triggering the DPV phenomenon among low  $q$  systems. Notoriously, the two W Serpentids in this sample are W Ser and  $\beta$  Lyr, both in the extreme of the mass distribution, again suggesting no link between DPVs and W Serpentids. A search in the literature reveals that some of the Algols with  $r_c < R_1 < r_{\max}$  show discs (e.g. SW Cyg, Richards et al. 2014; RX Gem, Olson & Etzel 2015) whereas others do not (e.g. TW And, Manzoori 2014; KO Aql, Soyduğan et al. 2007). This is consistent with the traditional view that they should show transient discs (Peters 2001). However, in this range DPVs have stable discs but are restricted to the ranges  $r_c < R_1 < r_{\max}$ ;  $7M_\odot < M_1 < 10M_\odot$  and  $8M_\odot < M_{\text{total}} < 13M_\odot$ . This range of parameters seems to be exclusive of the DPV phenomenon.

#### 4.1.2 Are DPV gainers Be stars?

Having determined luminosities, masses and temperatures for DPV gainers in Section 3.2, it is now clear that they share physical characteristics, including position in the HR diagram and possibly rapid rotation, with Be stars (e.g. Zorec, Frémat & Cidale 2005). We would like to rise the still speculative question whether DPV gainers are subject to the same mechanism producing stochastic mass ejections in Be stars, which is hitherto unknown (Rivinius, Carciofi and Martayan 2013). If the mechanism is synchronized with the orbit of a close stellar companion, it could produce regular mass ejections, producing the regular long-cycle variability typical of a DPV.

At least a fraction of Be stars showing long-term quasi-periodic variability can share with DPVs physical mechanisms inducing activity. More studies are needed to explore this possibility.

## 4.2 An evolutionary link between DPVs and W Serpentids?

The different regions occupied by W Serpentids and DPVs in Fig. 10 suggest an evolutionary link between both types of variables. In this Section we explore such a possibility considering the path followed by  $R_1/a$ ,  $q$  and the mass transfer rate  $\dot{M}$  during binary evolution. For that, we assume that the evolutionary history of DPVs and W Serpentis stars can be represented by the binary star evolutionary models described in Section 2.7. Moreover, we take one of these models as representative of the general evolution of the mass ratio,  $\dot{M}$  and primary fractional radius for the systems under study.

To illustrate the prediction of a model, let's consider HD 170582 (Mennickent et al. in preparation). This model was found among the grid of binary star evolutionary track by Van Rensbergen et al. (2011) following the method described by Mennickent et al. (2012a) and turned to be conservative with initial masses of  $6 M_\odot$  and  $2.4 M_\odot$  and initial orbital period of 1.0 day. The theoretical path  $R_1/a$  (Fig. 10) indicates that the system evolves from the upper right part of the diagram into the lower left part, lowering its mass ratio mainly due to the mass transfer happening during epochs of Roche-lobe overflow. The accompanying right panel shows the mass transfer rate as a function of  $R_1/a$  indicating that the maximum mass transfer rate occurs before reaching the critical radius (around fractional radius 0.27 in our example).

Accordingly, if W Serpentids are systems with larger  $\dot{M}$  than DPVs, as suggested by their larger variability, larger infrared excess and orbital period changes, and both kinds of systems are evolutionarily connected, then we should expect to find them above DPVs in the  $R_1 - q$  diagram, since they are hypothetically earlier in the evolutionary history (DPVs are found after the peak of mass transfer). Surprisingly, this is not the case, W Serpentis stars are found below DPVs. It is then possible that both kinds of objects are not linked by evolution.

In addition we note that W Serpentids span a mass range much wider than DPVs. Taking into account objects like RS Cep ( $M_{\text{tot}} = 3.2 M_\odot$ ) or SX Cas ( $M_{\text{tot}} = 6.6 M_\odot$ ) it is hard to imagine that these object can be DPV precursors since they cannot produce early B-type components (apparently a condition for a DPV) by mass exchange. In principle, they might be considered as the outcome of a previous DPV phase, if large systemic mass loss has happened in the system. However, to account for the primary mass of some W Serpentids, the gainer should loose mass, which seems highly unlikely. For the above reasons, we suspect that the less massive W Serpentids are not evolutionarily connected with DPVs. However, it is hard to be conclusive about the other more massive systems, for instance  $\beta$  Lyrae.

Finally in this section we notice that the possibility that the disc is formed before the tangential-impact condition is not possible for HD 170582, since the system comes from a higher mass ratio and larger fractional primary radius, i.e. from a zone where no disc is possible, as shown by the  $R_1/a$  track in Fig. 10.

## 5 CONCLUSIONS

In this paper we have reported the discovery of 7 new Galactic Double Periodic Variables and listed some properties of all 21 known

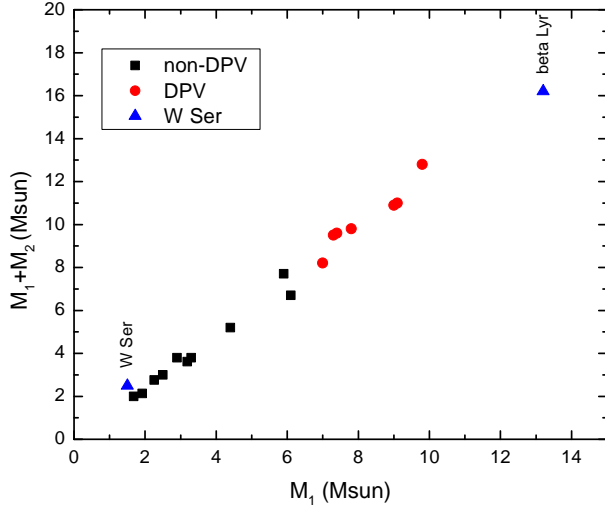


**Figure 11.** Primary mass and total mass of systems (Algols, DPVs and W Serpentids) with primaries with  $r_c < R_1 < r_{max}$ .

ones. We have also compared observational and physical parameters of W Serpentids and DPVs. Especially their infrared colors and properties of accretion discs were also studied. Whereas most of the 21 DPVs and 10 W Serpentids are included in the photometric study, only some of them have published physical data, making our study of physical characteristics still based on few cases, 7 DPVs and 7 W Serpentids. Keeping this low-number statistic restriction in mind, we arrive to the following conclusions:

- Galactic DPVs show a correlation between their long and orbital periods. The long period is roughly 33 times the orbital one, but a range of period ratios are observed, between 27 and 39.
- Among DPVs and W Serpentids, longer orbital period systems tend to show larger  $H - K$  and  $W2 - W3$  colors.
- Contrary to previous reports (probably affected by difficulties in determining eclipse timings in light curves with variable shape), we find a constant orbital period for the W Serpentis system UX Mon, viz.  $P_o = 5.90442$  days. We notice that the linear ephemerides for the main minimum remains valid for at least 59 years.
- In general, W Serpentids show larger infrared excess than DPVs. In both classes the excess, at least in some systems and excluding epochs of eclipses, is variable. We show that this can be understood in terms of variable amounts of circumstellar mass.
- Among our sample, the system with the largest  $H - K$  and  $W2 - W3$  color excess is BY Crucis.
- DPV primaries are tangential-impact systems, i.e. they are slightly above the Lubow-Shu radius and some of them might (if rotating critically) be barely inside the region of impact-systems. Surprisingly, all of them show rather stable discs.
- Discs of DPVs usually extend below the critical tidal radius.
- Discs of W Serpentids usually extend up to the critical tidal radius.
- Among impact systems, DPVs are those with primaries corresponding to slightly evolved B-type stars, with masses in the range  $7 M_\odot < M_1 \lesssim 10 M_\odot$ . They should rotate rapidly sharing physical characteristics with Be stars, which are B-type fast rotators surrounded by disc-like envelopes whose mass ejection mechanism is still unknown. In our sample the total mass of a DPV is in the range  $8 M_\odot < M_{total} < 13 M_\odot$ .

## 6 ACKNOWLEDGMENTS

We thank an anonymous referee whose comments helped to improve a first version of this manuscript. We also acknowledge Gorko Djurašević for useful discussions about this paper and Ahmet Dervişoğlu for providing comparison data. This publication makes use of VOSA, developed under the Spanish Virtual Observatory project supported from the Spanish MICINN through grant AyA2008-02156. This research has made use of the SIMBAD database, operated at CDS, Strasbourg, France. This publication makes use of data products from the Wide-field Infrared Survey Explorer, which is a joint project of the University of California, Los Angeles, and the Jet Propulsion Laboratory/California Institute of Technology, funded by the National Aeronautics and Space Administration. This research has made use of the NASA/IPAC Infrared Science Archive, which is operated by the Jet Propulsion Laboratory, California Institute of Technology, under contract with the National Aeronautics and Space Administration. This publication makes use of data products from the Two Micron All Sky Survey, which is a joint project of the University of Massachusetts and the Infrared Processing and Analysis Center/California Institute of Technology, funded by the National Aeronautics and Space Administration and the National Science Foundation. R.E.M. acknowledges support by VRID-Enlace 214.016.001-1.0 and the BASAL Centro de Astrofísica y Tecnologías Afines (CATA) PFB-06/2007. We acknowledge support from the Polish NCN grant 2011/03/B/ST9/02667 to ZK.

## REFERENCES

- Andersen J., Pavlovski K., Pirola V., 1989, *A&A*, 215, 272  
 Andersen J., Nordstrom B., Mayor M., Polidan R. S., 1988, *A&A*, 207, 37  
 Arnold C. N., Montle R. E., Stuhlinger T. W., Hall D. S., 1979, *AcA*, 29, 243  
 Atwood-Stone C., Miller B. P., Richards M. T., Budaj J., Peters G. J., 2012, *ApJ*, 760, 134  
 Barría D., Mennickent R. E., Schmidtbreick L., Djurašević G., Kołaczowski Z., Michalska G., Vučković M., Niemczura E., 2013, *A&A*, 552, A63  
 Bessell M. S., Castelli F., Plez B., 1998, *A&A*, 333, 231  
 Budding E., Erdem A., Çiçek C., Bulut I., Soyduğan F., Soyduğan E., Bakiş V., Demircan O., 2004, *A&A*, 417, 263  
 Bystrov N. F., Polojntsev D. D., Potter H. I., Yagudin L. I., Zallez R. F., Zelaya J. A., 1994, The final FOCAT-S star catalogue for southern hemisphere. *Bulletin d'Information du Centre de Donnees Stellaires*, Vol. 44, p. 3  
 Cannon A. J., Pickering E. C., 1922, *AnHar*, 97, 1  
 Dachs J., Kiehling R., Engels D., 1988, *A&A*, 194, 167  
 Daems K., Waelkens C., Mayor M., 1997, *A&A*, 317, 823  
 Dall T. H. et al., 2007, *A&A*, 470, 1201  
 de Mink S. E., Sana H., Langer N., Izzard R. G., Schneider F. R. N., 2014, *ApJ*, 782, 7  
 Dervişoğlu A., Tout C. A., Ibanoglu C., 2010, *MNRAS*, 406, 1071  
 Deschamps R., Braun K., Jorissen A., Siess L., Baes M., Camps P., 2015, *A&A*, 577, A55  
 Desmet M. et al., 2010, *MNRAS*, 401, 418  
 Djurašević G., 1993a, *Ap&SS*, 206, 129  
 Djurašević G., 1993b, *Ap&SS*, 208, 85  
 Djurašević G., Latković O., Vince I., Cséki A., 2010, *MNRAS*, 409, 329

**Table 2.** The Galactic Double Periodic Variables ordered by increasing orbital period. The ratio between long and orbital periods is given, along with published spectral type and extreme visual magnitudes. References are given for the spectral type and for the paper announcing the long period (V360 Lac) or DPV character. The single-wave (sw), double-wave (dw) or eclipsing (e) character of the orbital light curve is also given.

Object	Other name	ASAS or NSVS ID	RA (2000)	DEC (2000)	Max V (mag)	Min V (mag)	$P_o$ (days)	$P_l$ (days)	$P_l/P_o$	Type	SpT	Ref. SpT	Ref. DPV
HD 151582	TYC 7867-2398-1	ASAS 1164954-3832.7	16 49 54.27	-38 32 40.6	9.43	9.53	5.823	160	27.48	sw	B3II/IIIe	Houk (1982)	3
DQ Vel	TYC 8175-333-1	ASAS 1093034-5011.9	09 30 34.22	-50 11 54.1	10.73	11.69	6.0833	189	31.06	e	B3V+AIII	Barria et al. (2013)	1
BF Cir	HD 132461	ASAS 1150232-6457.7	15 02 32.02	-64 57 41.9	8.65	9.24	6.4592	219	33.87	dw	B5V	Houk & Cowley (1975)	3
GK Nor	TYC 8708-412-1	ASAS 1153451-5824.0	15 34 50.91	-53 45 46.5	11.13	11.90	6.53971	225	34.44	e	-	-	1
HD 135938	TYC 8695-2281-1	ASAS 1152008-5345.8	15 20 08.44	-53 45 46.5	9.13	9.38	6.6477	231	34.78	dw	B5/B6IVp	Houk & Cowley (1975)	1
HD 50526	TYC 161-1014-1	ASAS J065402-0648.8	06 54 02.03	+06 48 48.8	8.12	8.48	6.7007	192	28.61	dw	B9	Ochsenbein (1980)	1
V1001 Cen	HIP 69978	ASAS J1141910-5552.9	14 19 09.04	-55 52 56.1	7.20	7.37	6.736	247	36.97	dw	B4IV/V+OB:	Dall et al. (2007)	3
NSV 16849	HD 256413	ASAS J062402+1954.5	06 24 01.82	+19 54 32.3	8.87	9.02	6.775	242	34.83	dw	B5III	Jaschek et al. (1964)	3
HD 90834	TYC 8613-1865-1	ASAS 102742-5917.3	10 27 41.61	-59 17 04.9	9.08	9.42	6.815	231	33.90	dw	B5/B6III/IV(e)	Houk & Cowley (1975)	1
TYC 5985-958-1	GSC 05985-00958	ASAS 1074415-1758.8	07 44 15.30	-17 58 45.7	10.4	10.75	7.4054	229	30.87	dw	-	-	1
TYC 8627-1591-1	CPD-583114	ASAS 1110629-5848.3	11 06 29.07	-58 48 18.8	8.77	8.94	7.462	268	35.92	dw	B5	Wallenquist (1931)	3
V393 Sco	HIP 87191	ASAS 1174848-3503.5	17 48 47.60	-35 03 25.6	7.39	8.31	7.71259	253	32.79	e	B3III	Houk (1982)	1
V761 Mon	HIP 36093	ASAS 1072610-1032.9	07 26 09.54	-10 32 56.7	8.25	8.45	7.754	268	34.71	dw	B5V+A:	Houk (1999)	3
CZ Cam	HIP 18593	NSVS 512654	03 58 43.64	+69 00 59.5	9.37	9.66	8.055	266	33.03	dw	B5	Heckmann (1975)	3
TYC 5978-472-1	CPD-212186	ASAS 1072641-2208.9	07 26 41.41	-22 08 53.7	10.20	10.73	8.2958	312	37.61	dw	B3V	Munch (1952)	1
LP Ara	HD 328568	ASAS 1164002-4639.6	16 40 01.78	-46 39 34.9	10.00	10.98	8.53295	273	31.99	e	B8	Nesterov et al. (1995)	1
V360 Lac	HIP 112778	ASAS 1183048-1447.5	22 30 21.77	+44 57 12.2	5.88	5.99	10.085	322	31.95	dw	B3e+F9IV	Hill et al. (1997)	4
AU Mon	HIP 33237	ASAS 1065455-0122.5	06 54 54.71	-01 22 32.8	8.20	9.16	11.1309	421	37.84	e	B5e+G	Desmet et al. (2010)	1
HD 170582	TYC 5703-2382-1	ASAS 1183048-1447.5	18 30 47.53	-14 47 27.8	9.60	9.86	16.871	537	31.83	dw	A3III:	Cannon & Pickering (1922)	1
V4142 Sgr	HD 317151	ASAS 1180745-2824.1	18 07 44.56	-28 24 04.3	10.85	12.70	30.636	1206	39.36	e	A0	Nesterov et al. (1995)	2
V495 Cen	CD-55 4911	ASAS 1130135-5605.5	13 01 34.81	-56 05 30.9	9.82	10.88	33.4873	1283	38.31	e	Be+G2ep	Skiff (2014)	2

Ref. DPV: (1) Mennickent et al. 2012a, (2) Mennickent & Rosales 2014, (3) this paper, (4) Hill et al. 1997

**Table 3.** Physical parameters for Galactic DPVs and the LMC system OGLE 05155332-6925581 (iDPV). We give donor and gainer masses and radii ( $M_c$ ,  $M_h$  and  $R_c$ ,  $R_h$ , respectively), the total system mass ( $M_{tot}$ ), the mass ratio ( $q$ ), the donor and gainer effective temperatures ( $T_c$  and  $T_h$ , respectively), the logarithm of their luminosities in terms of the solar luminosity ( $\log(L_c/L_\odot)$  and  $\log(L_h/L_\odot)$ , respectively), the system age, the hydrogen fraction of the stellar core for the donor ( $X_c$ ) and the gainer ( $X_h$ ) and the system mass transfer rate ( $\dot{M}$ ). The last four parameters in this table are from the models that best fit the observations. In all models the mass transfer rate ( $\dot{M}$ ) is the same that the mass accretion rate. Errors can be found in the references. The systems are sorted by total mass.

DPV	$M_c$ ( $M_\odot$ )	$M_h$ ( $M_\odot$ )	$M_{tot}$ ( $M_\odot$ )	$q$	$R_c$ ( $R_\odot$ )	$R_h$ ( $R_\odot$ )	$T_c$ (K)	$T_h$ (K)	$\log(L_c/L_\odot)$	$\log(L_h/L_\odot)$	age (yr)	$X_c$	$X_h$	$\dot{M}$ ( $M_\odot \text{ yr}^{-1}$ )	ref
LP Ara	3.0	9.8	12.8	0.30	11.6	5.3	9500	16400	2.99	3.26	-	-	-	-	7
iDPV	1.9	9.1	11.0	0.21	8.9	5.6	12900	25100	3.26	4.02	4.8E7	0.0	0.5	3.1E-6	1
HD 170582	1.9	9.0	10.9	0.21	15.6	5.5	8000	18000	2.94	3.46	7.7E7	0.0	0.5	1.6E-6	5
V393 Sco	2.0	7.8	9.8	0.25	9.4	4.1	7950	15850	2.46	3.06	7.0E7	0.1	0.6	9.5E-9	2
V360 Lac	1.2	7.4	9.6	0.16	8.8	7.6	6000	18000	2.11	3.54	-	-	-	<3.2E-6	6
DQ Vel	2.2	7.3	9.5	0.31	8.4	3.6	9350	18600	2.66	3.14	7.4E7	0.1	0.5	9.8E-9	3
AU Mon	1.2	7.0	8.2	0.17	10.1	5.1	5750	15900	1.98	3.14	2.0E8	0.0	0.3	7.6E-6	4,8

References: (1) Garrido et al. 2013, (2) Mennickent et al. 2012a, (3) Barria et al. 2013, (4) Mennickent 2014, (5) Mennickent et al. 2015, (6) Linnell et al. 2006, (7) Mennickent et al. 2010, (8) Djurašević et al. 2010.

Eggleton P., 2006, Evolutionary processes in binary and multiple stars, Cambridge Astrophysical Series 40, Cambridge University Press.

Garrido H. E., Mennickent R. E., Djurašević G., Kołaczowski Z., Niemczura E., Mennekens N., 2013, MNRAS, 428, 1594

Georgy C., Meynet G., Maeder A., 2011, A&A, 527, A52

Griffin R. E., 2002, AJ, 123, 988

Gudel, M. & Elias, II, N. M. 1996, in Astronomical Society of the Pacific Conference Series, Vol. 93, Radio Emission from the Stars and the Sun, ed. A. R. Taylor & J. M. Paredes, 312

Halbedel E. M., 1989, PASP, 101, 995

Harmanec P., et al., 1996, A&A, 312, 879

Heckmann O., 1975, AGK 3. Star catalogue of positions and proper motions north of -2.5 deg. declination, Hamburg-Bergedorf: Hamburger Sternwarte, edited by Dieckvoss W.

Hessman F. V., Hopp U., 1990, A&A, 228, 387

Hill G., Harmanec P., Pavlovski K., Bozic H., Hadrava P., Koub-sky P., Ziznovsky J., 1997, A&A, 324, 965

Houk N., Cowley A. P., 1975, Dept. of Astronomy, Univ. of Michigan Ann Arbor, Catalogue of two dimensional spectral types for the HD stars, Vol. 1

Houk N., 1982, Dept. of Astronomy, Univ. of Michigan Ann Arbor, Catalogue of two-dimensional spectral types for the HD stars, Vol. 3

Houk N., Swift C., 1999, Dept. of Astronomy, Univ. of Michigan Ann Arbor, Catalogue of two-dimensional spectral types for the HD stars, Vol. 5

Howells L., Steele I. A., Porter J. M., Etherton J., 2001, A&A, 369, 99

Hutchings J. B., van Heteren J., 1981, PASP, 93, 626

Jaschek C., Conde H., de Sierra A.C., 1964, Catalogue of Stellar Spectra Classified in the Morgan-Keenan System, Serie Astronomica, No 2., La Plata: Observatorio Astronomico de la Universidad de la Plata

Kalv P., 1979, TarOT, 58, 3

Koch R. H., Guinan E. F., 1978, IBVS, 1483, 1

Kondo Y., McCluskey G. E., Jr., Parsons S. B., 1985, ApJ, 295, 580

Kreiner J. M., Ziolkowski J., 1978, AcA, 28, 497

Linnell A. P., et al., 2006, A&A, 455, 1037

Lubow S. H., Shu F. H., 1975, ApJ, 198, 383

Lucy L. B., 2005, A&A, 439, 663

Manzoori D., 2014, AN, 335, 1064

Mennickent R. E., Pietrzyński G., Diaz M., Gieren W., 2003, A&A, 399, L47

Mennickent R. E., Kołaczowski Z., Michalska G., Pietrzyński G., Gallardo R., Cidale L., Granada A., Gieren W., 2008, MNRAS, 389, 1605

**Table 4.** Physical parameters and additional data of W Ser stars. Labels are as in Table 3 and spectral types are from SIMBAD except for RY Per (Olson & Plavec 1997), SX Cas (Andersen et al. 1988) and RS Cep (Olson & Etzel 1995). The systems are sorted by total mass.

system	$P_o$ (d)	$M_c$ ( $M_\odot$ )	$M_h$ ( $M_\odot$ )	$M_{tot}$ ( $M_\odot$ )	$q$	$R_c$ ( $R_\odot$ )	$R_h$ ( $R_\odot$ )	$T_c$	$T_h$	$\log(L_c/L_\odot)$	$\log(L_h/L_\odot)$	$\dot{M}/\dot{P}$ ( $M_\odot \text{ yr}^{-1}/(\text{s yr}^{-1})$ )	Sp	ref
$\beta$ Lyr	12.94	3.0	13.2	16.2	0.22	15.2	6.0	13200	30200	3.81	4.42	1.6E-5/18.93	B8II-IIIep	1
BY Cru	106.4	1.7	9.1	10.8	0.19	52	-	11000	-	4.55	-	-/-	F0Ib-II	7
W Cru	198.5	1.2	7.8	9.0	0.16	76	4.0	5500	14000	3.68	2.74	4.4E-8-1.3E-7/	G2Iab	4
RY Per	6.86	1.6	6.2	7.8	0.26	8.10	4.06	6250	18000	1.98	3.21	-/-	B4:V+F7:II-III	3
RX Cas	32.33	1.8	5.8	7.6	0.30	23.5	2.5	4400	-	2.29	-	6E-6/19.86	K1III+A5eIII	5
V367 Cyg	18.6	3.3	4.0	7.3	0.82	21.3	2.9	10400	14800	3.68	2.56	5-7E-5/	B8peIa+F4III	11
UX Mon	5.90	3.9	3.4	7.3	1.15	9.80	3.49	5990	13000	2.04	-	-/-	A3	2
SX Cas	36.6	1.5	5.1	6.6	0.29	23.5	3.0	4000	-	2.10	-	-4.8	A6(shell)+K3III	6
RS Cep	12.42	0.4	2.8	3.2	0.14	7.63	2.65	4610	9400	1.37	1.69	-/-	B9.7eV+G8III	8
W Ser	14.17	1.0	1.5	2.5	0.64	1.00	1.34	-	-	-0.21	0.45	/14	F5III	9,10

References: (1) Mennickent & Djurašević 2013. (2) Sudar et al. 2011, (3) Olson & Plavec 1997, (4) Zoła 1996, (5) Andersen et al. 1989, (6) Andersen et al. 1988, (7) Daems et al. 1997, (8) Olson & Etzel 1995, (9) Budding et al. 2004, (10) Koch & Guinan (1978), (11) Zoła & Ogłóza 2001.

**Table 5.** Errors for some of the physical parameters given in Tables 3 and 4.

system	$eM_c$ ( $M_\odot$ )	$eM_h$ ( $M_\odot$ )	$eM_{tot}$ ( $M_\odot$ )	$eq$	$eR_c$ ( $R_\odot$ )	$eR_h$ ( $R_\odot$ )	$eT_c$ (K)	$eT_h$ (K)
LP Ara	-	-	-	-	-	-	-	-
iDPV	0.20	0.50	0.54	0.02	0.30	0.20	500	-
HD 170582	0.10	0.20	0.22	0.01	0.20	0.20	100	1500
V393 Sco	0.20	0.50	0.54	0.03	0.30	0.20	300	500
V360 Lac	0.05	0.30	0.30	0.01	-	-	200	1000
DQ Vel	0.20	0.30	0.36	0.03	0.20	0.20	100	500
AU Mon	0.20	0.30	0.36	0.03	0.50	0.50	-	-
$\beta$ Lyr	0.30	0.30	0.40	0.02	0.20	0.20	-	-
BY Cru	-	-	-	-	-	-	-	-
W Cru	-	-	-	0.03	-	-	-	-
RY Per	0.10	0.16	0.19	0.01	0.17	0.14	-	-
RX Cas	0.40	0.50	0.60	0.07	1.20	-	-	-
UX Mon	0.29	0.40	0.49	0.10	0.03	0.05	200	1000
SX Cas	0.40	0.40	0.60	0.08	1.30	0.40	300	-
RS Cep	-	-	-	-	-	-	-	-
W Ser	-	-	-	-	-	-	-	-
V367 Cyg	0.90	0.50	1.00	0.30	2.00	-	-	-

Mennickent R. E., Kołaczowski Z., Graczyk D., Ojeda J., 2010, MNRAS, 405, 1947

Mennickent R. E., Graczyk D., Kołaczowski Z., Michalska G., Barría D., Niemczura E., 2011, IAUS, 272, 527

Mennickent R. E., Djurašević G., Kołaczowski Z., Michalska G., 2012a, MNRAS, 421, 862

Mennickent R. E., Kołaczowski Z., Niemczura E., Diaz M., Cure M., Araya I., Peters G., 2012b, MNRAS, 427, 607

Mennickent R. E., Djurašević G., 2013, MNRAS, 432, 799

Mennickent R. E., 2014, PASP, 126, 821

Mennickent R. E., Rosales J., 2014, IBVS, 6116, 1

Mennickent R. E., Djurašević G., Cabezas M., Cséki A., Rosales J. G., Niemczura E., Araya I., Curé M., 2015, MNRAS, 448, 1137

Münch L., 1952, Boletín de los Observatorios de Tonantzintla y Tacubaya Vol. 1 Num. 2, p. 1

Nesterov V. V., Kuzmin A. V., Ashimbaeva N. T., Volchkov A. A., Roeser S., Bastian U., 1995, A&AS, 110, 367, The Henry Draper Extension Charts: A catalogue of accurate positions, proper motions, magnitudes and spectral types of 86933 stars

Ochsenbein F., 1980, Bull. Inf. CDS, 19, 74

Olson E. C., Etzel P. B., 1994, AJ, 108, 262

Olson E. C., Etzel P. B., 1995, AJ, 110, 2385

Olson E. C., Plavec M. J., 1997, AJ, 113, 425

Olson E. C., Etzel P. B., 2015, AJ, 149, 125

Packet W., 1981, A&A, 102, 17

Paczynski B., 1977, ApJ, 216, 822

Parihar P., Messina S., Bama P., Medhi B. J., Muneer S., Velu C., Ahmad A., 2009, MNRAS, 395, 593

Pawlak M., et al., 2013, AcA, 63, 323

Perryman M. A. C., et al., 1997, A&A, 323, L49

Peters G. J., 2001, ASSL, 264, 79

Plavec, M., 1980a, "The impact of IUE on Binary Star Studies", U.C.L.A. Astronomy and Astrophysics Preprint No. 95.

Plavec, M., 1980b, "Mass loss from Interacting Close Binary Systems", U.C.L.A. Astronomy and Astrophysics Preprint No. 112.

Plavec M. J., 1982, NASCP, 2338, 526

Plavec M. J., Weiland J. L., Koch R. H., 1982, ApJ, 256, 206

Plavec M. J., Dobias J. J., 1983, ApJ, 272, 206

Plavec M. J., 1989, SSRv, 50, 95

Plavec M. J., 1989, SSRv, 50, 95

Pojmanski G., 2002, Acta Astronomica, 52, 397

**Table 6.** Mean WISE magnitudes for Double Periodic Variables. The number of averaged measures and the variance of the mean are also given. Epoch is given in julian day minus 2 400 000.

Object	Epoch	NW1	W1	eW1	NW2	W2	eW2	NW3	W3	eW3	NW4	W4	eW4
V393 Sco	55273.9	10	6.3863	0.0133	11	6.3843	0.0094	9	6.2888	0.0043	10	6.1727	0.0282
HD 50526	55285.5	12	7.6418	0.0063	13	7.6082	0.0071	11	7.5064	0.0066	11	7.3702	0.0696
LP Ara	55260.0	3	8.6070	0.0058	7	8.6206	0.0055	3	8.4633	0.0489	3	-	-
HD 90834	55208.6	8	8.5485	0.0171	10	8.3591	0.0131	10	8.3660	0.0094	11	7.0731	0.0584
HD 90834	55382.7	15	8.3586	0.0155	14	8.2610	0.0163	15	8.2265	0.0126	17	7.0882	0.0810
GK Nor	55252.1	4	9.4543	0.0054	4	9.4425	0.0114	5	9.5876	0.0962	8	7.7174	0.0297
CZ Cam	55255.9	8	7.2654	0.0061	9	7.1439	0.0121	9	6.9609	0.0112	9	6.6589	0.0475
AU Mon	55286.4	12	7.4262	0.0071	14	7.3321	0.0072	14	7.0826	0.0072	14	6.7645	0.0667
V1001 Cen	55240.2	12	6.6881	0.0084	13	6.6575	0.0072	13	6.5844	0.0035	14	6.4391	0.0251
DQ Vel	55357.5	3	8.9337	0.0088	3	8.8813	0.0049	4	8.8182	0.0319	15	7.5678	0.0614
V495 Cen	55226.4	11	7.4510	0.0101	14	7.3351	0.0079	12	6.9176	0.0063	13	6.3630	0.0307
V495 Cen	55406.6	12	7.3406	0.0041	14	7.1981	0.0068	11	6.8238	0.0039	13	6.2637	0.0350
BF Cir	55251.1	14	7.3446	0.0138	9	7.2959	0.0171	5	7.2282	0.0057	11	6.8606	0.0289
TYC 5978-472-1	55298.8	10	8.9348	0.0050	11	8.8644	0.0047	12	8.7053	0.0146	12	7.3874	0.0826
HD 135938	55248.7	11	8.1606	0.0039	12	8.1215	0.0053	12	7.9824	0.0055	11	7.1285	0.0653
HD 151582	55260.6	11	7.9816	0.0038	11	7.9063	0.0093	8	7.7578	0.0067	9	7.4073	0.0601
HD 170582	55283.1	11	7.7867	0.0113	11	7.7081	0.0088	10	7.5881	0.0072	10	7.0755	0.0549
TYC 5985-958-1	55302.8	11	9.7673	0.0044	12	9.7267	0.0054	17	9.5016	0.0239	13	7.5242	0.0697
TYC 8627-1591-1	55213.2	15	8.1965	0.0048	15	8.1963	0.0079	16	8.2111	0.0090	15	7.4741	0.0690
TYC 8627-1591-1	55388.6	15	8.1066	0.0038	15	8.1043	0.0042	15	8.1004	0.0046	16	7.5813	0.0441
V761 Mon	55296.1	13	7.6085	0.0060	14	7.5079	0.0063	14	7.2911	0.0044	14	6.9685	0.0460

**Table 7.** Mean WISE magnitudes for W Serpentis stars. The number of averaged measures and the variance of the mean are also given. Epoch is given in julian day minus 2 400 000.

Object	Epoch	NW1	W1	eW1	NW2	W2	eW2	NW3	W3	eW3	NW4	W4	eW4
W Ser	55278.3	10	4.9480	0.0049	9	4.5058	0.0214	11	3.9167	0.0056	11	3.3055	0.0068
W Cru	55221.7	16	6.0051	0.0223	17	5.7672	0.0150	13	5.2522	0.0067	15	4.8000	0.0103
W Cru	55401.1	15	5.5384	0.0164	16	5.1005	0.0270	16	4.8562	0.0106	17	4.3814	0.0100
SX Cas	55213.6	10	6.0058	0.0161	10	5.8752	0.0128	10	5.6539	0.0043	11	5.2675	0.0102
SX Cas	55401.1	16	5.9231	0.0037	19	5.8127	0.0086	17	5.6208	0.0027	19	5.2316	0.0106
RX Cas	55247.1	9	5.3727	0.0203	10	5.0776	0.0280	8	4.9386	0.0075	8	4.5903	0.0147
RY Per	55235.7	4	7.7963	0.0085	4	7.7548	0.0080	5	7.6586	0.0087	8	6.4769	0.0346
UX Mon	55304.1	4	6.9363	0.0059	3	6.9037	0.0180	3	6.6957	0.0224	5	6.3780	0.0525
RS Cep	55266.3	20	8.4906	0.0038	19	8.4586	0.0056	18	8.1620	0.0090	19	7.4905	0.0413
BY Cru	55223.5	15	4.0338	0.0063	15	2.8843	0.0407	13	1.4884	0.0129	15	0.7556	0.0076
BY Cru	55403.3	18	4.1393	0.0115	18	2.8846	0.0484	18	1.5982	0.0113	16	0.7499	0.0064
V367 Cyg	55339.1	13	4.7850	0.0271	17	4.4098	0.0320	12	3.8147	0.0161	12	2.6889	0.0087

Poleski R., Soszyński I., Udalski A., Szymański M. K., Kubiak M., Pietrzyński G., Wyrzykowski Ł., Ulaczyk K., 2010, *AcA*, 60, 179

Pols O. R., Schröder K.-P., Hurley J. R., Tout C. A., Eggleton P. P., 1998, *MNRAS*, 298, 525

Puss A., Leedjarv L., 1997, *BaltA*, 6, 395

Pustynnik I., Kalv P., Harvig V., Aas T., 2007, *A&AT*, 26, 339

Quiroga C., Mikołajewska J., Brandi E., Ferrer O., García L., 2002, *A&A*, 387, 139

Richards M. T., Cocking A. S., Fisher J. G., Conover M. J., 2014, *ApJ*, 795, 160

Rivinius T., Carciofi A. C., Martayan C., 2013, *A&ARv*, 21, 69

Sarna M. J., 1993, *MNRAS*, 262, 534

Simon V., 1997, *A&A*, 319, 886

Skiff B. A., 2014, *Catalogue of Stellar Spectral Classifications*, VizieR On-line Data Catalog: B/mk. Originally published in: Lowell Observatory (October 2014)

Skrutskie M. F., et al., 2006, *AJ*, 131, 1163

Soydugan F., Frasca A., Soydugan E., Catalano S., Demircan O., İbanoğlu C., 2007, *MNRAS*, 379, 1533

Stellingwerf R. F., 1978, *ApJ*, 224, 953

Sudar D., Harmanec P., Lehmann H., Yang S., Božić H., Ruždjak D., 2011, *A&A*, 528, A146

Szczygiel D. M., Socrates A., Paczynski B., Pojmanski G., Pilecki B., 2008, *Acta Astronomica*, 58, 405

Tarasov A. E., Berdyugina S. V., Berdyugin A. V., 1998, *AstL*, 24, 316

van Rensbergen W., De Greve J. P., De Loore C., Mennekens N., 2008, *yCat*, 348, 71129

Van Rensbergen W., de Greve J. P., Mennekens N., Jansen K., de Loore C., 2011, *A&A*, 528, A16

Wallenquist A., 1931, *Annalen v.d. Bosscha-Sterrenwacht*, Vol. 3, 3. gedeelte, Bandoeng: Nix, 1931, p. C3

Warner B., 1995, *Cambridge Astrophysics Series*, 28

Weiland J. L., Shore S. N., Beaver E. A., Lyons R. W., Rosenblatt E. I., 1995, *ApJ*, 447, 401



**Table 8.** Mean WISE magnitudes for the sample of Be stars studied by Howells et al. (2001). The number of averaged magnitudes and the variance of the mean are also given. Epoch is given in julian day minus 2 400 000.

Object	Epoch	NW1	W1	eW1	NW2	W2	eW2	NW3	W3	eW3	NW4	W4	eW4
BD+05 3704	55281.8	11	6.1935	0.0141	12	6.2083	0.0095	12	6.2894	0.0030	11	6.2140	0.0142
BD+17 4087	55309.4	13	9.5734	0.0044	13	9.5957	0.0041	12	9.5604	0.0180	13	7.4322	0.0363
BD+20 4449	55316.7	12	8.6632	0.0033	14	8.7186	0.0070	13	8.7003	0.0075	13	6.8136	0.0498
BD+21 4695	55349.7	15	5.6497	0.0117	15	5.2739	0.0159	4	4.6550	0.0064	3	3.7037	0.0167
BD+23 1148	55270.5	9	6.5306	0.0098	10	6.5203	0.0055	10	6.5312	0.0065	11	6.3644	0.0643
BD+27 797	55265.1	24	7.2760	0.0070	24	6.9868	0.0050	24	6.2142	0.0034	24	5.1681	0.0170
BD+27 850	55267.1	11	8.8902	0.0051	9	8.9197	0.0037	11	8.9821	0.0346	11	7.4075	0.0717
BD+27 3411	55307.7	19	3.0899	0.0942	18	2.4064	0.1232	14	4.4551	0.0031	17	3.6030	0.0169
BD+28 3598	55317.7	17	6.6895	0.0239	18	6.8596	0.0073	17	6.9085	0.0048	17	6.7999	0.0405
BD+29 3842	55317.7	18	8.7521	0.0050	18	8.7720	0.0057	16	8.8202	0.0095	18	7.6491	0.0671
BD+29 4453	55345.7	14	7.1104	0.0104	14	6.7790	0.0083	12	5.8019	0.0030	10	4.2240	0.0077
BD+30 3227	55287.3	19	6.8265	0.0081	20	6.8709	0.0047	19	6.9060	0.0039	17	6.7951	0.0433
BD+31 4018	55325.9	15	5.9698	0.0080	16	5.5746	0.0201	16	4.9844	0.0038	16	4.3699	0.0172
BD+36 3946	55327.4	18	6.2966	0.0081	19	5.9652	0.0113	17	5.2534	0.0030	17	4.4509	0.0094
BD+37 675	55234.6	11	5.9765	0.0113	11	5.8060	0.0147	11	5.3981	0.0050	11	4.5746	0.0071
BD+37 3856	55328.7	19	9.3122	0.0043	19	9.3522	0.0073	18	8.8134	0.0222	18	6.6343	0.0386
BD+40 1213	55261.6	10	6.5136	0.0115	12	6.3053	0.0058	11	5.7150	0.0050	12	4.9535	0.0099
BD+42 1376	55267.1	11	7.0121	0.0096	12	6.8702	0.0065	11	6.0722	0.0049	12	4.9454	0.0086
BD+42 4538	55375.6	17	7.4583	0.0084	15	7.1718	0.0019	17	6.1395	0.0047	17	4.9861	0.0110
BD+43 1048	55257.1	11	8.3699	0.0054	11	8.1750	0.0089	11	7.5406	0.0080	11	6.7283	0.0598
BD+45 933	55254.0	11	7.3565	0.0086	12	7.3815	0.0056	12	7.3992	0.0096	12	6.4274	0.0460
BD+46 275	55217.6	9	4.3324	0.0151	9	4.1378	0.0256	6	4.3095	0.0049	7	3.9483	0.0123
BD+46 275	55405.9	15	4.3300	0.0068	14	4.1499	0.0216	13	4.3540	0.0044	12	4.0987	0.0064
BD+47 183	55214.4	13	3.9720	0.0065	13	3.3056	0.0351	13	2.8178	0.0056	13	1.9732	0.0086
BD+47 183	55402.1	14	3.9733	0.0098	14	3.4179	0.0305	12	2.8296	0.0040	11	1.9809	0.0066
BD+47 857	55243.9	13	3.6515	0.0117	13	3.0137	0.0305	12	2.4723	0.0109	11	1.6250	0.0079
BD+47 939	55251.5	13	3.5626	0.0133	13	2.9694	0.0433	5	2.4942	0.0245	6	1.6977	0.0115
BD+47 3985	55381.1	35	4.9382	0.0093	34	4.4169	0.0147	27	3.7499	0.0028	34	2.8551	0.0049
BD+49 614	55231.3	12	7.5282	0.0038	13	7.4612	0.0061	13	6.8310	0.0050	13	5.9392	0.0201
BD+50 825	55246.5	20	5.8037	0.0092	26	5.7168	0.0106	21	5.3420	0.0065	24	4.5349	0.0095
BD+50 3430	55367.1	19	6.8457	0.0075	22	6.7068	0.0071	20	6.0545	0.0049	21	5.1320	0.0101
BD+51 3091	55365.8	21	6.0315	0.0137	25	5.9576	0.0072	23	5.8773	0.0030	23	5.2602	0.0141
BD+55 552	55233.8	15	7.8254	0.0053	15	7.6070	0.0047	15	7.0055	0.0051	16	6.2826	0.0237
BD+55 605	55235.5	14	9.3514	0.0064	13	9.3702	0.0053	15	9.1095	0.0214	15	7.3985	0.0692
BD+55 2411	55356.3	31	5.8959	0.0078	34	5.8246	0.0090	32	5.7749	0.0031	32	5.2688	0.0080
BD+56 473	55234.8	13	8.1258	0.0062	14	7.9419	0.0063	13	7.1418	0.0064	14	6.0912	0.0231
BD+56 478	55234.6	28	7.0385	0.0080	26	6.7960	0.0052	28	6.3310	0.0028	28	5.7736	0.0139
BD+56 484	55234.7	14	7.8384	0.0057	14	7.5403	0.0079	15	6.7193	0.0061	15	5.8327	0.0253
BD+56 493	55234.8	30	8.7677	0.0036	32	8.6562	0.0033	32	8.3571	0.0064	32	7.4324	0.0426
BD+56 511	55235.0	13	7.9062	0.0039	15	7.7807	0.0049	13	7.2805	0.0064	15	6.5809	0.0577
BD+56 573	55235.5	14	6.6435	0.0132	15	6.1040	0.0090	15	5.3573	0.0057	14	4.8395	0.0121
BD+57 681	55241.7	29	7.3277	0.0068	29	7.3072	0.0057	29	7.3073	0.0045	28	7.1215	0.0526
BD+58 554	55242.8	14	8.1644	0.0040	14	8.0739	0.0055	14	7.4791	0.0052	13	6.5668	0.0397
BD+58 2320	55378.5	25	8.4337	0.0077	26	8.2460	0.0070	25	7.6126	0.0062	24	7.1105	0.0537
CD-22 13183	55284.6	22	6.9400	0.0045	22	6.8234	0.0046	22	6.1277	0.0040	22	5.2087	0.0140
CD-28 14778	55283.8	11	7.7360	0.0034	11	7.4631	0.0053	11	6.6760	0.0032	11	5.7842	0.0262
CD-27 11872	55272.9	18	5.8685	0.0222	18	5.6379	0.0128	16	4.9731	0.0027	22	3.9635	0.0093
CD-27 16010	55338.5	17	4.3160	0.0086	16	4.0098	0.0267	15	3.9422	0.0061	14	3.2371	0.0060
BD-12 5132	55285.3	11	7.1323	0.0174	12	6.8462	0.0065	10	6.0340	0.0058	11	5.2101	0.0143
BD-19 5036	55282.9	12	6.9371	0.0088	13	6.9588	0.0053	13	7.0665	0.0055	10	7.1262	0.0939
BD-02 5328	55317.3	9	6.3130	0.0075	11	6.2670	0.0099	11	5.8419	0.0036	11	4.9435	0.0117
BD-01 3834	55305.8	8	7.1134	0.0076	10	6.7531	0.0068	9	5.9466	0.0036	10	5.1152	0.0119

Whipple F. L., 1966, Smithsonian Astrophysical Observatory Star Catalog. Smithsonian Institution Press, Washington

Wilson R. E., Rafert J. B., Markworth N. L., 1984, IAPPP, 16, 1

Wozniak P. R. et al., 2004, AJ, 127, 2436

Wright, E. L., Eisenhardt, P. R. M., Mainzer, A. K., et al. 2010, AJ, 140, 1868

Yoo K. H., 2008, NewA, 13, 646

Young A., Snyder J. A., 1982, ApJ, 262, 269

Zahn J. P., 1977, A&A, 57, 383

Zahn J. P., 1975, A&A, 41, 329

Zoła S., 1996, A&A, 308, 785

Zoła S., Ogłóza W., 2001, A&A, 368, 932

Zorec J., Frémat Y., Cidale L., 2005, A&A, 441, 235

**Table 9.** Mean WISE magnitudes and spectral types for a sample of non-variable Hipparcos stars. The number of WISE averaged magnitudes and the variance of the mean are also given.

HIP	NW1	W1	eW1	NW2	W2	eW2	NW3	W3	eW3	NW4	W4	eW4	SpType
57	15	6.1905	0.0142	15	6.2239	0.0105	15	6.2224	0.0042	15	6.1145	0.0237	K2V
594	15	8.5200	0.0052	16	8.5381	0.0053	16	8.5099	0.0093	2	7.6230	0.0863	A9V
1585	13	8.2686	0.0049	12	8.2950	0.0058	13	8.2590	0.0118	3	7.6167	0.1158	G2V
1837	30	6.0640	0.0088	29	6.0820	0.0123	29	6.1111	0.0058	30	5.8806	0.0192	K3/K4V
2107	11	7.3050	0.0056	13	7.3325	0.0051	11	7.3356	0.0034	10	7.1229	0.0482	G2/G3V
2964	13	7.4816	0.0055	14	7.5044	0.0061	14	7.5005	0.0069	8	7.2986	0.0900	F0V
3553	10	7.7460	0.0060	11	7.7802	0.0052	11	7.7622	0.0063	5	7.5634	0.1554	G3V
4537	14	7.3291	0.0107	14	7.3343	0.0037	13	7.3496	0.0042	12	7.1597	0.0750	F5V
5130	16	7.9609	0.0044	17	7.9916	0.0060	16	7.9589	0.0062	5	7.5070	0.0684	F8V
5462	38	7.0895	0.0048	40	7.1257	0.0035	40	7.0906	0.0029	40	6.7136	0.0254	G5V
5755	16	8.6863	0.0052	16	8.7153	0.0075	16	8.7153	0.0132	0	-	-	B8V
5935	14	7.4049	0.0073	14	7.4471	0.0064	13	7.4411	0.0041	10	7.2664	0.0668	F5V
6169	15	7.5973	0.0072	14	7.5991	0.0048	15	7.5949	0.0069	12	7.2745	0.0723	F5V
6664	13	8.2403	0.0058	14	8.2729	0.0072	13	8.2825	0.0094	3	7.5690	0.1673	A8V
6672	17	8.3842	0.0048	18	8.4011	0.0042	18	8.3796	0.0056	5	7.4748	0.1496	A3V
8167	25	8.5554	0.0033	23	8.5894	0.0030	23	8.5380	0.0088	5	7.3620	0.1372	F5V
8373	13	8.2312	0.0058	14	8.2704	0.0058	13	8.2801	0.0091	2	7.7360	0.0438	G3V
9499	19	6.4809	0.0086	21	6.5066	0.0074	19	6.4913	0.0049	20	6.4727	0.0291	F7/8V
10360	11	7.7695	0.0053	11	7.7849	0.0075	10	7.7763	0.0070	7	7.4310	0.0783	F0V
13089	20	7.7264	0.0042	19	7.7323	0.0047	21	7.7242	0.0044	9	7.4800	0.0656	A9V
13285	12	7.5673	0.0062	12	7.5822	0.0042	12	7.5495	0.0062	7	7.2986	0.0350	G0V
15493	16	7.3433	0.0072	14	7.3863	0.0040	12	7.3515	0.0060	12	7.2620	0.0533	K0V
16465	11	8.3055	0.0055	11	8.3431	0.0052	9	8.3350	0.0076	4	7.5252	0.0817	A3V
16595	46	7.7703	0.0022	46	7.8192	0.0035	46	7.7668	0.0035	26	7.4697	0.0584	G5/G6V
17280	13	8.7922	0.0055	12	8.8215	0.0075	11	8.7695	0.0086	4	7.6240	0.0701	B9V
18719	9	6.8560	0.0087	9	6.9259	0.0101	9	6.9242	0.0027	9	6.8512	0.0679	G4V
19210	18	7.3509	0.0050	19	7.3670	0.0034	17	7.3604	0.0060	16	7.3072	0.0583	F5V
20019	18	6.4029	0.0085	14	6.3946	0.0182	13	6.3875	0.0074	21	6.2680	0.0297	G8V
20088	15	7.9141	0.0049	15	7.9505	0.0061	15	7.9247	0.0076	6	7.4895	0.0831	G1V
21159	10	7.9726	0.0080	10	7.9919	0.0086	8	8.0635	0.0104	3	7.5603	0.1435	B5V
21472	14	7.7242	0.0055	15	7.7513	0.0073	13	7.7296	0.0070	11	7.4577	0.0588	A0V
21498	13	8.1855	0.0037	14	8.1990	0.0044	12	8.1846	0.0068	6	7.6347	0.0766	F0V
22037	34	7.4060	0.0038	32	7.4141	0.0036	31	7.3943	0.0035	29	7.0341	0.0353	F0V
22295	30	6.8008	0.0063	30	6.8253	0.0035	31	6.8186	0.0039	32	6.5332	0.0199	F7V
23373	18	6.7974	0.0123	17	6.8061	0.0041	17	6.8210	0.0046	17	6.8294	0.0536	F7V
24922	14	8.4860	0.0055	14	8.5041	0.0085	13	8.4059	0.0100	7	7.3923	0.0672	B8V
25108	15	7.1920	0.0083	15	7.2328	0.0047	15	7.2418	0.0042	15	7.1533	0.0507	F5/F6V
25321	14	6.3347	0.0088	15	6.3759	0.0085	15	6.3903	0.0038	14	6.2974	0.0291	G8V
27102	11	7.9664	0.0077	12	7.9914	0.0082	12	7.9475	0.0123	8	7.5802	0.0595	B9V
27185	12	6.5821	0.0162	12	6.6044	0.0048	13	6.6986	0.0041	13	6.5483	0.0456	G2V
28247	23	7.7193	0.0030	25	7.7732	0.0046	23	7.7308	0.0045	17	7.4963	0.0756	G6/G8V
28923	17	8.9858	0.0046	18	9.0223	0.0048	17	9.0076	0.0131	3	7.7953	0.0729	B8/B9V
29644	15	6.7397	0.0092	15	6.8147	0.0060	13	6.8060	0.0077	12	6.7253	0.0309	G8V
30729	12	6.6851	0.0049	17	6.7240	0.0057	18	6.7273	0.0031	18	6.4988	0.0757	G5V
31036	12	7.2713	0.0103	10	7.2863	0.0057	11	7.3113	0.0058	13	7.1449	0.0786	F2V
32235	43	7.2850	0.0045	44	7.3144	0.0032	42	7.2705	0.0032	43	7.1295	0.0404	G6V
32326	10	7.2229	0.0088	10	7.2516	0.0073	10	7.2445	0.0051	10	7.2051	0.0629	G2/G3V
33208	14	9.2631	0.0040	17	9.3046	0.0058	14	9.2994	0.0113	2	7.6840	0.1520	B3V
34205	13	8.3539	0.0039	14	8.3788	0.0059	14	8.3548	0.0085	3	7.7450	0.1039	A8V
34230	11	6.8207	0.0139	12	6.8555	0.0061	11	6.7825	0.0059	11	6.7073	0.0617	G5V
35117	15	9.1273	0.0052	15	9.1751	0.0052	13	9.1855	0.0124	2	7.0925	0.2493	B9V
36827	22	6.0054	0.0123	22	6.0195	0.0173	12	5.9892	0.0050	20	5.7438	0.0221	K2V
36944	9	8.9640	0.0051	10	9.0097	0.0097	9	9.0436	0.0106	0	-	-	B3V
39687	20	8.7628	0.0055	19	8.8032	0.0044	19	8.8583	0.0093	1	7.8330	0.0000	B8V
41587	20	7.4709	0.0056	20	7.4871	0.0038	18	7.4880	0.0042	15	7.4312	0.0951	G3V
43386	73	8.3713	0.0075	77	8.4064	0.0072	73	8.4143	0.0086	21	7.6716	0.0473	B8V
43562	14	8.1879	0.0031	14	8.2033	0.0033	14	8.1690	0.0082	7	7.5341	0.0490	F8/G0V
44101	15	7.2011	0.0071	15	7.2319	0.0060	15	7.2151	0.0060	15	7.1778	0.0543	K1V
44258	14	8.4189	0.0047	12	8.4395	0.0036	14	8.4435	0.0123	0	-	-	A1V
44526	20	6.2976	0.0046	26	6.3929	0.0050	25	6.3851	0.0037	26	6.2088	0.0172	K2V
45009	12	7.7062	0.0104	12	7.7256	0.0067	9	7.6978	0.0077	7	7.4709	0.0536	A0V

**Table 10.** Mean WISE magnitudes and spectral types for a sample of non-variable Hipparcos stars. The number of WISE averaged magnitudes and the variance of the mean are also given.

HIP	NW1	W1	eW1	NW2	W2	eW2	NW3	W3	eW3	NW4	W4	eW4	SpType
45857	16	7.9026	0.0057	16	7.9387	0.0068	15	7.9277	0.0094	8	7.5949	0.0700	F6V
47163	16	6.9721	0.0100	16	6.9927	0.0056	15	7.0032	0.0046	15	7.0963	0.0515	G0V
47743	14	7.8848	0.0029	12	7.9023	0.0051	15	7.9281	0.0104	8	7.3515	0.0909	A2V
48141	15	7.0227	0.0089	16	7.0600	0.0051	16	7.0543	0.0045	14	6.9986	0.0708	G8V
48627	16	7.6642	0.0052	15	7.6421	0.0066	14	7.6209	0.0061	12	7.4146	0.0811	F0V
49269	15	8.5885	0.0064	14	8.6186	0.0047	14	8.6057	0.0093	5	7.6614	0.0596	B9V
49636	13	9.1161	0.0054	12	9.1346	0.0064	12	9.1838	0.0130	1	7.7590	0.0000	A0V
49913	34	6.9441	0.0058	35	6.9949	0.0043	31	6.9919	0.0026	33	7.0311	0.0404	G1V
50718	13	8.0399	0.0038	13	8.0797	0.0049	13	8.0400	0.0054	6	7.5937	0.0843	G3V
51534	16	7.7429	0.0055	18	7.7469	0.0060	15	7.7412	0.0104	10	7.4347	0.0839	F0V
52511	14	8.0116	0.0060	14	8.0154	0.0068	12	8.0171	0.0095	4	7.4727	0.0553	F2V
52706	22	6.1241	0.0096	26	6.1397	0.0057	19	6.1563	0.0028	25	6.0932	0.0110	G8V
52716	20	6.9832	0.0073	19	7.0058	0.0061	18	7.0082	0.0047	19	7.0499	0.0509	F7V
52787	11	6.3790	0.0091	13	6.4629	0.0083	13	6.4546	0.0037	12	6.4153	0.0367	K0V
53651	29	7.2672	0.0056	30	7.2957	0.0029	27	7.2985	0.0033	29	7.2931	0.0403	F8/G0V
55457	39	6.5985	0.0063	43	6.5951	0.0035	42	6.6297	0.0030	43	6.5545	0.0250	F3V
56264	18	8.6274	0.0044	17	8.6710	0.0043	17	8.6861	0.0118	2	7.8680	0.0559	B6V
57427	16	8.5301	0.0034	16	8.5724	0.0049	15	8.5067	0.0101	2	7.6910	0.1584	B9V
59315	11	6.4349	0.0098	13	6.4614	0.0085	12	6.4708	0.0037	12	6.2839	0.0243	G5V
60679	14	7.3088	0.0116	14	7.3833	0.0073	13	7.3445	0.0051	11	7.2857	0.0705	K0V
63009	13	7.2270	0.0104	12	7.2648	0.0026	12	7.2548	0.0049	12	7.1032	0.0834	G5V
63861	12	7.8967	0.0054	13	7.9258	0.0049	14	7.8940	0.0081	6	7.4772	0.0895	G5V
63862	11	6.6898	0.0071	12	6.7437	0.0057	13	6.7282	0.0044	13	6.7325	0.0593	G5V
64075	16	8.6369	0.0042	13	8.6577	0.0052	16	8.6921	0.0113	2	7.7045	0.0244	B9V
65315	10	7.4352	0.0068	10	7.4614	0.0031	11	7.4535	0.0067	8	7.3440	0.1039	G5V
65186	25	8.2238	0.0043	24	8.2691	0.0028	25	8.2799	0.0084	21	7.0522	0.0481	B8V
67065	19	7.5635	0.0063	19	7.5832	0.0056	13	7.6118	0.0050	10	7.4691	0.0835	F0V
67191	12	7.1253	0.0132	11	7.1240	0.0076	11	7.1471	0.0077	10	7.0243	0.0679	F2/F3V
67466	16	8.6491	0.0043	16	8.6614	0.0053	16	8.7285	0.0132	5	7.6896	0.0791	B9V
67907	16	6.9468	0.0131	16	7.0071	0.0056	17	7.0500	0.0058	15	6.9987	0.0432	G0V
69023	16	8.5389	0.0044	15	8.5537	0.0047	15	8.6191	0.0118	1	7.6620	0.0000	F0V
70477	14	8.2305	0.0042	12	8.2635	0.0035	14	8.3207	0.0079	13	7.4325	0.0598	B4V
71666	14	9.0378	0.0049	13	9.0673	0.0060	14	9.1400	0.0168	0	-	-	B3V
72816	16	7.9609	0.0032	16	7.9915	0.0044	16	8.0381	0.0088	9	7.4046	0.0810	B5Vn
74294	20	8.5834	0.0046	19	8.6008	0.0042	18	8.6158	0.0080	2	7.7030	0.0849	A2V
75183	17	7.8358	0.0054	18	7.8781	0.0046	17	7.8541	0.0067	8	7.3822	0.0594	G0V
78299	15	7.2287	0.0072	14	7.2601	0.0054	13	7.2687	0.0053	13	7.1797	0.0540	F3V
80320	11	7.6194	0.0101	10	7.6345	0.0057	11	7.5530	0.0085	9	7.1217	0.0956	G2/G3V
80341	11	7.3750	0.0075	11	7.3951	0.0089	11	7.4414	0.0087	9	7.2601	0.0790	F2V
80535	11	7.1501	0.0094	10	7.1481	0.0062	10	7.1727	0.0076	10	7.1865	0.0663	G0V
81334	12	7.4137	0.0077	12	7.4323	0.0080	12	7.4588	0.0098	9	7.1768	0.0989	F2V
82447	24	6.3267	0.0090	23	6.3477	0.0092	20	6.3794	0.0049	21	6.3005	0.0260	G3/G5V
82551	22	8.1692	0.0049	6	8.1875	0.0044	17	8.1355	0.0116	4	7.5727	0.0974	A9V
82577	16	8.3354	0.0055	16	8.3573	0.0051	15	8.3667	0.0078	6	7.7397	0.0667	B9V
84703	11	7.4937	0.0064	11	7.4916	0.0058	12	7.5183	0.0061	7	7.3931	0.0476	F0V
85516	13	8.8232	0.0038	14	8.8399	0.0049	13	8.8098	0.0119	3	7.7613	0.0684	F0V
87292	15	6.9561	0.0109	16	7.0026	0.0052	15	6.9752	0.0055	15	6.9105	0.0602	K3V
88289	14	8.2190	0.0058	14	8.2473	0.0045	15	8.2463	0.0097	4	7.5765	0.1043	A0V
89907	10	8.0257	0.0031	11	8.0618	0.0049	12	8.0516	0.0079	7	7.4346	0.0833	F0V
93227	12	7.7947	0.0053	12	7.8174	0.0060	12	7.8254	0.0068	9	7.4704	0.0714	F0V
94626	15	8.4136	0.0043	15	8.4280	0.0058	14	8.4084	0.0123	3	7.7793	0.0330	F0/F2V
95243	24	8.5514	0.0031	13	8.5670	0.0042	12	8.5198	0.0120	3	7.6757	0.1085	A9V
96303	26	7.0499	0.0067	28	7.0560	0.0058	28	7.0345	0.0048	26	6.8211	0.0336	A5V
99092	38	5.9763	0.0102	32	5.9977	0.0063	28	5.9656	0.0023	30	5.9360	0.0160	K0V
99412	19	8.3470	0.0045	19	8.3953	0.0059	17	8.4829	0.0099	0	-	-	B1V
104580	20	7.5069	0.0063	19	7.5125	0.0033	19	7.5121	0.0047	7	7.2757	0.0640	F5V
104691	60	8.3692	0.0026	58	8.3792	0.0029	56	8.3345	0.0043	25	7.6545	0.0459	F3/F5V
105620	9	7.0793	0.0074	9	7.1117	0.0068	9	7.0972	0.0059	10	6.8834	0.0593	G6V
107385	11	7.3453	0.0046	12	7.4013	0.0048	13	7.3595	0.0061	13	7.3830	0.0530	K2V
108480	14	7.8047	0.0042	14	7.8454	0.0051	14	7.7986	0.0072	10	7.4160	0.0431	G2V

**Table 11.** Mean WISE magnitudes and spectral types for a sample of non-variable Hipparcos stars. The number of WISE averaged magnitudes and the variance of the mean are also given.

HIP	NW1	W1	$eW1$	NW2	W2	$eW2$	NW3	W3	$eW3$	NW4	W4	$eW4$	SpType
110659	19	7.1374	0.0079	20	7.1784	0.0059	22	7.1553	0.0039	20	6.9695	0.0364	G2V
111252	33	7.6631	0.0093	35	7.6702	0.0073	25	7.6841	0.0062	20	7.5951	0.0445	A2V
112825	30	8.0623	0.0029	30	8.0977	0.0029	30	8.0462	0.0055	13	7.6444	0.0478	F6V
113071	11	8.5904	0.0069	11	8.6048	0.0056	11	8.6101	0.0174	4	7.3853	0.0555	A1V
113701	12	6.2458	0.0173	12	6.2460	0.0107	12	6.2789	0.0046	12	6.2347	0.0298	K1V
114198	10	7.4420	0.0108	10	7.4582	0.0069	10	7.4404	0.0090	8	7.3285	0.0512	F0/F2V
114879	14	7.3284	0.0065	15	7.3596	0.0048	15	7.3639	0.0037	14	7.3174	0.0639	F0V
114997	29	7.5807	0.0050	29	7.5979	0.0035	28	7.5829	0.0046	21	7.4086	0.0490	F0V
115034	31	7.5080	0.0037	32	7.5127	0.0047	32	7.5438	0.0052	24	7.3797	0.0494	A6V
115694	16	7.7596	0.0051	16	7.7808	0.0031	16	7.7750	0.0069	9	7.4123	0.0651	F6/F7V
116122	26	6.8153	0.0064	26	6.8475	0.0029	27	6.8439	0.0036	28	6.7234	0.0336	G2V
116944	12	8.5752	0.0052	12	8.5886	0.0071	12	8.6220	0.0085	3	7.7160	0.1045	B7V
117086	10	7.9788	0.0093	9	7.9999	0.0045	9	7.9633	0.0060	4	7.5338	0.0761	F0V
117596	19	6.4351	0.0195	19	6.4310	0.0071	18	6.4336	0.0045	17	6.2812	0.0238	G3V
118056	12	7.3900	0.0034	12	7.4242	0.0057	10	7.4119	0.0043	11	7.2281	0.0483	F7V

**Table 12.** Primary radius, disc radius, binary separation and their errors. Stellar and orbital data are from Tables 3, 4 and 5 and references therein. Disc data are from references listed in Tables 3, 4 and 5, except for RX Cas (Djurašević 1993a), SX Cas (Djurašević 1993b) and W Ser (Weiland et al. 1995).

System	Type	$R_1$ ( $R_\odot$ )	$e(R_1)$ ( $R_\odot$ )	$R_d$ ( $R_\odot$ )	$e(R_d)$ ( $R_\odot$ )	$a$ ( $R_\odot$ )	$e(a)$ ( $R_\odot$ )	$R_d/a$	$e(R_d/a)$	$R_1/a$	$e(R_1/a)$
LP Ara	DPV	5.30	-	-	-	41.1	-	-	-	0.13	-
HD 170582	DPV	5.50	0.20	20.80	0.30	61.2	0.2	0.34	0.01	0.09	0.00
iDPV	DPV	5.60	0.20	14.10	0.50	35.2	0.5	0.40	0.02	0.16	0.01
V360 Lac	DPV	7.50	-	-	-	41.8	-	-	-	0.18	-
AU Mon	DPV	5.10	0.50	12.70	0.60	42.1	0.4	0.30	0.02	0.12	0.01
V393 Sco	DPV	3.60	0.20	9.70	0.30	35.1	0.5	0.28	0.01	0.10	0.01
DQ Vel	DPV	3.60	0.20	12.90	0.30	29.7	0.3	0.43	0.01	0.12	0.01
W Cru	WSer	4.00	-	126.00	-	299.0	-	0.44	-	0.01	-
RX Cas	WSer	2.50	-	18.80	-	40.0	-	0.47	-	0.06	-
SX Cas	WSer	3.00	0.40	37.00	-	87.1	-	0.42	-	0.03	-
$\beta$ Lyrae	WSer	6.00	0.20	28.30	0.30	58.5	0.3	0.48	0.01	0.10	0.00
UX Mon	WSer	3.49	0.05	9.20	1.00	26.7	0.7	0.34	0.05	0.13	0.01
W Ser	WSer	0.97	-	5.20	-	17.2	-	0.30	-	0.06	-
V367 Cyg	WSer	2.90	-	23.30	2.50	59.60	5.50	0.39	0.08	0.05	-

This paper has been typeset from a  $\text{\LaTeX}$  file prepared by the author.